FINAL REPORT WY2504F

Wyoming Department of Transportation

State of Wyoming

EVALUATION OF CONCRETE BRIDGE DECK MIXTURES USING SHRINKAGE-RING TESTS

By:

Department of Civil and Architectural Engineering
University of Wyoming
1000 East University Avenue, Dept. 3295
Laramie, WY 82071

July 2025

Notice

This document is disseminated under the sponsorship of the Wyoming Department of Transportation (WYDOT) in the interest of information exchange. WYDOT assumes no liability for the use of the information contained in this document. WYDOT does not endorse products or manufacturers. Trademarks or manufacturers' names appear in this report only because they are considered essential to the objective of the document.

Quality Assurance Statement

WYDOT provides high-quality information to serve Government, industry, and the public in a manner that promotes public understanding. Standards and policies are used to ensure and maximize the quality, objectivity, utility, and integrity of its information. WYDOT periodically reviews quality issues and adjusts its programs and processes to ensure continuous quality improvement. Further, if the report contains either confidential information or, if any information in the report is subject to copyright, patent, or trademark requirements, the report must contain additional disclaimers that may be obtained through the Research Center.

Creative Commons

Copyrighted works

Copyright and Proprietary Information

requires such. Prior use of the material in a WYDOT or governmental publication does not necessarily constitute permission to use it in a later publication.

- Courtesy — Acknowledgment or credit will be given by footnote, bibliographic reference, or a statement in the text for use of material contributed or assistance provided even when a copyright notice is not applicable.
- Caveat for Unpublished Work —Some material may be protected under common law or equity even though no copyright notice is displayed on the material. Credit will be given and permission will be obtained as appropriate.

Proprietary Information — To avoid restrictions on the availability of reports, proprietary information will not be included in reports unless it is critical to the understanding of a report and prior approval is received from WYDOT and the contractor. Reports containing such proprietary information will contain a statement on the Technical Report Documentation Page restricting availability and a notice on how to request a copy of the material.

No Generative Artificial Intelligence Training

Without any way limiting the author or other copyright owner's exclusive right under copyright, the owner of this report, which includes the authors, contractor and WYDOT, does not consent to the content being used or downloaded for the purposes of developing, training, or operating any artificial intelligence (AI) tool or model, or other machine learning systems operated by any generative artificial intelligence (GAI) model, which could include but is not limited to machine learning (ML) tools, large language models (LLM), generative adversarial networks (GAN), open AI programs (OpenAI), generative pre-trained transformers (GPT), or their sublicensees. Any use of this publication to train generative AI technologies or their sublicenses is expressly prohibited. The owner of this report reserve all rights to license uses of this work and any artificial intelligence tool that is capable of generating works must obtain the owner's specific and express permission to generate any works using data and information from this report.
Generative Artificial Intelligence (GAI) tools were used in the writing of this report, production of images and/or graphical elements, or in the collection and analysis of data. In order to be transparent in disclosing the materials and methods (or similar section) of this report, the author sets out at the end of the report which GAI tools were used. Authors understand they are fully responsible for the content of their report, even those parts produced by any GAI tools, and are thus liable for any breach of publication ethics.
Portions of the document may have been generated through the use of any GAI tool, but the ideas and underlying intent are created by a human author. AI may have been used to improve grammar and organization but not in creating the content of the report.

TECHNICAL REPORT DOCUMENTATION PAGE

1. Report No. WY2504F	**2. Government Accession No.**	**3. Recipient's Catalog No.**
4. Title and Subtitle Evaluation Of Concrete Bridge Deck Mixtures Using Shrinkage-Ring Tests		**5. Report Date** **6. Performing Organization Code:** University of Wyoming
7. Author(s) Shamel Perez Buenfil - 0000-0003-0010-6473 John Higgins - 0000-0002-2736-7633 Cesar Gerardo Freyre Pinto – 0000-0002-4288-4583 Jennifer Tanner Eisenhauer - 0000-0003-2433-2897		**8. Performing Organization Report No.**
9. Performing Organization Name and Address University of Wyoming Department of Civil and Architectural Engineering University of Wyoming, Dept 3295 Laramie, WY 82071-3295		**10. Work Unit No.** **11. Contract or Grant No.** **RS0221** https://ror.org/00pqdc111
12. Sponsoring Agency Name and Address Wyoming Department of Transportation 5300 Bishop Blvd Cheyenne, WY 82009-3340 WYDOT Research Center (307) 777-4182		**13. Type of Report and Period** Final Report **14. Sponsoring Agency Code** WYDOT
15. Supplementary Notes All restrictions for this report are set out in the disclaimer. WYDOT Project Manager: Whitney Wise		
16. Abstract The durability of concrete structures is dependent on the restrained shrinkage behavior of the mix: therefore, evaluating mixtures with different aggregates and mitigation measures is critical. The aim of this document is to evaluate and compare concrete mixture designs using granite and limestone aggregates in combination with different mitigation methods. The mitigation measures evaluated in this work are synthetic macrofibers, shrinkage reducing admixture (SRA), and internal curing (IC). A total of sixteen batches were tested, including individual and combined mitigation strategies using both aggregate types. Two experimental approaches were used to assess restrained shrinkage: single ring and dual ring according to AASTHO T334 and AASTHO T363, respectively. Mechanical properties such as compressive and tensile strength were studied for each mixture. Results indicated that limestone performs better than granite, but the statistical analysis showed that the effect of the aggregate is not significant. For single mitigation measures, internal curing is the most effective at delaying cracking. Incorporating fibers into the mixture roughly doubles the time to crack. Adding SRA into the mix increased the cracking age by 90 percent. The combination of IC with SRA proved to be the most effective measure for extending cracking time.		
17. Key Words Wyoming, Concrete, Shrinkage, Fibers, Shrinking Reducing Admixture, Internal Curing, Lightweight Fine Aggregate.	**18. Distribution Statement** This document is available through the National Transportation Library and the Wyoming State Library. Copyright ©.2017 All rights reserved, State of Wyoming, Wyoming Department of Transportation, the University of Wyoming, and the Tanner Research Group.	

19. Security Classif. (of this report) Unclassified	**20. Security Classif. (of this page)** Unclassified	**21. No. of Pages** 67	**22. Price**

Form DOT F 1700.7 (8-72) Reproduction of completed page authorized.

SI* (MODERN METRIC) CONVERSION FACTORS

APPROXIMATE CONVERSIONS TO SI UNITS

Symbol	When You Know	Multiply By	To Find	Symbol
		LENGTH		
in	inches	25.4	millimeters	mm
ft	feet	0.305	meters	m
yd	yards	0.914	meters	m
mi	miles	1.61	kilometers	km
		AREA		
in^2	square inches	645.2	square millimeters	mm^2
ft^2	square feet	0.093	square meters	m^2
yd^2	square yard	0.836	square meters	m^2
ac	acres	0.405	hectares	ha
mi^2	square miles	2.59	square kilometers	km^2
		VOLUME		
fl oz	fluid ounces	29.57	milliliters	mL
gal	gallons	3.785	liters	L
ft^3	cubic feet	0.028	cubic meters	m^3
yd^3	cubic yards	0.765	cubic meters	m^3
		NOTE: volumes greater than 1000 L shall be shown in m^3		
		MASS		
oz	ounces	28.35	grams	g
lb	pounds	0.454	kilograms	kg
T	short tons (2000 lb)	0.907	megagrams (or "metric ton")	Mg (or "t")
		TEMPERATURE (exact degrees)		
°F	Fahrenheit	5 (F-32)/9 or (F-32)/1.8	Celsius	°C
		ILLUMINATION		
fc	foot-candles	10.76	lux	lx
fl	foot-Lamberts	3.426	$candela/m^2$	cd/m^2
		FORCE and PRESSURE or STRESS		
lbf	poundforce	4.45	newtons	N
lbf/in^2	poundforce per square inch	6.89	kilopascals	kPa

APPROXIMATE CONVERSIONS FROM SI UNITS

Symbol	When You Know	Multiply By	To Find	Symbol
		LENGTH		
mm	millimeters	0.039	inches	in
m	meters	3.28	feet	ft
m	meters	1.09	yards	yd
km	kilometers	0.621	miles	mi
		AREA		
mm^2	square millimeters	0.0016	square inches	in^2
m^2	square meters	10.764	square feet	ft^2
m^2	square meters	1.195	square yards	yd^2
ha	hectares	2.47	acres	ac
km^2	square kilometers	0.386	square miles	mi^2
		VOLUME		
mL	milliliters	0.034	fluid ounces	fl oz
L	liters	0.264	gallons	gal
m^3	cubic meters	35.314	cubic feet	ft^3
m^3	cubic meters	1.307	cubic yards	yd^3
		MASS		
g	grams	0.035	ounces	oz
kg	kilograms	2.202	pounds	lb
Mg (or "t")	megagrams (or "metric ton")	1.103	short tons (2000 lb)	T
		TEMPERATURE (exact degrees)		
°C	Celsius	1.8C+32	Fahrenheit	°F
		ILLUMINATION		
lx	lux	0.0929	foot-candles	fc
cd/m^2	$candela/m^2$	0.2919	foot-Lamberts	fl
		FORCE and PRESSURE or STRESS		
N	newtons	0.225	poundforce	lbf
kPa	kilopascals	0.145	poundforce per square inch	lbf/in^2

TABLE OF CONTENTS

LIST OF FIGURES

LIST OF TABLES

LIST OF ACRONYMS

AASHTO – American Association of State Highway and Transportation Officials
ACI – American Concrete Institute
ANOVA – Analysis of variance
ASTM – American Society for Testing and Materials
CA – Coarse aggregate
F- Fibers
F8 – Fiber content of 8 pounds per cubic yard
FA – Fine aggregate
GR – Granite
IC – Internal Curing
LS – Limestone
LW – Lightweight
LWA – Lightweight Aggregates
LWFA – Lightweight Fine Aggregate
MPa – Megapascal
NHST – Null Hypothesis Significance Testing
PDF – Probability density function
S2 – Shrinkage reducing admixture content of 2 percent
SRA – Shrinkage Reducing Admixture
SSD – Saturated surface-dry
STC - Self-Temperature Compensation
US – United States
UW - University of Wyoming
WYDOT - Wyoming Department of Transportation

EXECUTIVE SUMMARY

The aim of this document is to evaluate and compare concrete using granite and limestone aggregates in combination with different mitigation methods. The mitigation measures evaluated in this work are synthetic macrofibers, shrinkage reducing admixture (SRA), and internal curing. A total of sixteen batches were tested, including individual and combined mitigation strategies using both aggregate types.

Two experimental approaches were used to assess restrained shrinkage: single ring and dual ring according to (American Association of State Highway and Transportation Officials) AASTHO T334 and T363, respectively. Mechanical properties such as compressive and tensile strength were studied for each mixture. Results indicated that incorporating fibers into the mixture roughly doubles the time to cracking. Adding Shrinkage Reducing Admixture (SRA) into the mix increased the cracking age by 90 percent. The combination of 8 lb/yd^3 (4.75 kg/m^3) of fibers with 2 percent of SRA replacement proved to be the most effective measure for extending cracking time, improving it by an average of five times the original cracking. The most effective single mitigation measure is internal curing.

1 INTRODUCTION

Concrete is a heterogeneous material composed of coarse aggregate, fine aggregate, cement and water. The use of water and cement creates a paste that gains strength over time. By controlling the ratio of these two materials we can achieve a wide range of strengths. Different concrete properties have been studied such as compressive strength, tensile strength, modulus of elasticity, and the relations between them. However, there is more to learn about behavior during the curing process. As concrete goes through this process, it will be subjected to volumetric changes. If the concrete is restrained during these changes, and the internal stresses exceed the tensile strength, this will result in early-age cracking. In the context of bridges, cracks can lead to corrosion and decrease the deck's lifespan. Currently, the cost of maintenance of concrete on bridge decks represents a significant part of Wyoming DOT's budget. It is necessary to further understand the reasons why shrinkage occurs and, subsequently, to evaluate the best practices to mitigate concrete shrinkage to prevent cracking.

The combined production of limestone and granite make up about 50 percent of the total aggregate production in the United States (US) (Langer, 2011). Because of this, both limestone and granite are extensively used as aggregates in concrete, and they play an important role in the overall performance of concrete mixtures. On the other hand, there are new strategies that have been developed to mitigate shrinking in concrete mixtures. The incorporation of fibers, SRA, and internal curing have shown to effectively reduce shrinkage in concrete structures.

There are different standards that evaluate time to cracking of restrained concrete mixtures. One of the most used methods is AASHTO T334, which determines the cracking tendency of restrained concrete specimens in a controlled environment. However, there is a relatively new method, AASTHO T363, that also evaluates cracking potential in concrete with a more complex restraint system that can also evaluate expansion. Although both tests have being used to evaluate restrained shrinkage, there is no direct comparison between both setups. This gap suggests that further investigation can be beneficial to evaluate the practicality of future testing.

Despite the well-established knowledge of shrinkage's impact on durability, it is important to mitigate this issue. This project evaluates the effectiveness of different methods in reducing shrinkage.

1.1 Research Objectives

The objectives of this proposal are as follows:

- Evaluate the effects of single methods to mitigate shrinkage.
- Quantify the beneficial effects of multiple methods to mitigate shrinkage.
- Propose solutions for WYDOT using standard mix designs for two types of aggregates; and
- Provide guidance on the use of internal curing for concrete mix designs.

1.2 Report Overview

Chapter 1 Introduces the research.
Chapter 2 Provides detailed relevant literature on concrete shrinkage and mitigation methods.
Chapter 3 Addresses the materials used throughout the study, their physical and mechanical properties, as they apply.
Chapter 4 Describes the test methods and equipment used in this research.
Chapter 5 Demonstrates the results of the single-ring and dual-ring tests, compressive and tensile strength tests.
Chapter 6 Presents the conclusions of this research and the recommendations for future work.

2 LITERATURE REVIEW

Concrete is widely utilized due to its versatility, strength, durability, and affordability. During the curing process, concrete is subjected to volumetric changes. Part of the serviceability requirements involve controlling cracking. If the concrete is restrained, tensile stresses are induced that could result in early-age cracking (Zhan & He, 2019a). Cracks can lead to corrosion and decrease the structure lifespan. It is essential to further understand the reasons why shrinkage occurs, and, subsequently, to evaluate best practices to mitigate concrete shrinkage.

2.1 Types of Shrinkage

Concrete shrinkage can be classified as autogenous, plastic, drying, carbonation, and thermal shrinkage; each has its own characteristics and causes (Elzokra et al., 2020). The total shrinkage can be divided into two types: early-age and long-term shrinkage (Lofgren & Esping, 2006). Early-age shrinkage can be attributed to drying, thermal, or autogenous shrinkage; long-term shrinkage is associated with those three types plus carbonation shrinkage (Holt, 2001). Early-age shrinkage occurs when concrete is more vulnerable because it has not yet developed its full tensile strain capacity, making it more susceptible to cracking (Holt & Leivo, 2004).

About 60 percent of the total shrinkage occurs within the first few days after casting (Kurup et al., 2024). The bulk of shrinkage is due to autogenous and drying shrinkage (Hyodo et al., 2013), however, in conventional concrete, drying shrinkage is the main mechanism contributing to overall shrinkage (Sakata & Shimomura, 2004), as shown in Figure 1, and it will be discussed in the following section, Autogenous Shrinkage. Autogenous, drying, and thermal shrinkage can occur at both early and later stages, causing overlap between them and adding their effects into cracking (Wu et al., 2017).

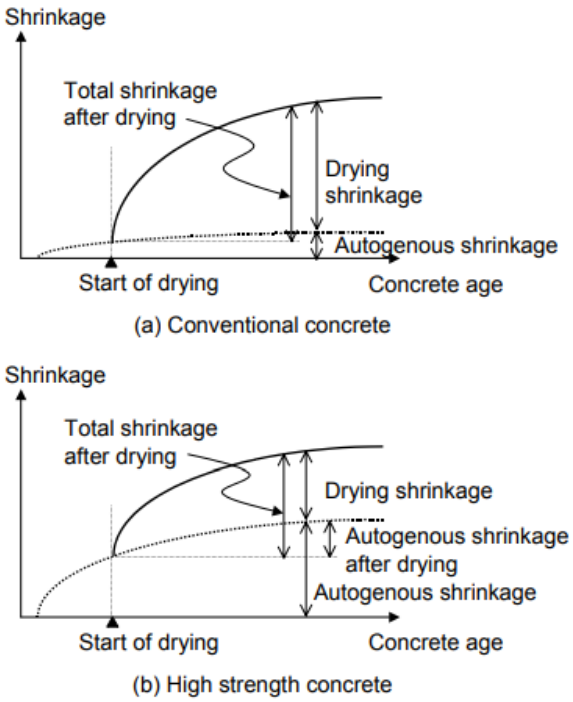

Figure 1. Shrinkage in conventional and high-strength concrete. Source: Sakata & Shimomura (2004).

2.1.1 Autogenous Shrinkage

Autogenous shrinkage of cement pastes results in volume change caused by chemical reactions during hydration. Temperature variation and water loss are not part of this type of shrinkage. Autogenous shrinkage is determined by several variables such as cement chemical composition, fineness of cement, water/cement ratio, reaction temperature, and presence of admixtures (Van Breugel, 1998). It is necessary to study how these parameters can reduce volume changes associated with this type of shrinkage to avoid micro-cracking during the hardening process.

Autogenous shrinkage is smaller than the total shrinkage. It has been shown that autogenous shrinkage of low water-cement ratio concretes can reach the same values as drying shrinkage while the difference increases as the water-cement ratio increases as well (Tazawa & Miyazawa, 1995). A 2018 study showed that for regular-strength concretes of 30 MPa, autogenous shrinkage is approximately 25 percent of the total shrinkage. On the other hand, high-strength concrete showed that roughly 50 percent of the total strain was due to autogenous shrinkage by comparing the right sides of Figure 2 a and b (Gilbert et al., 2018).

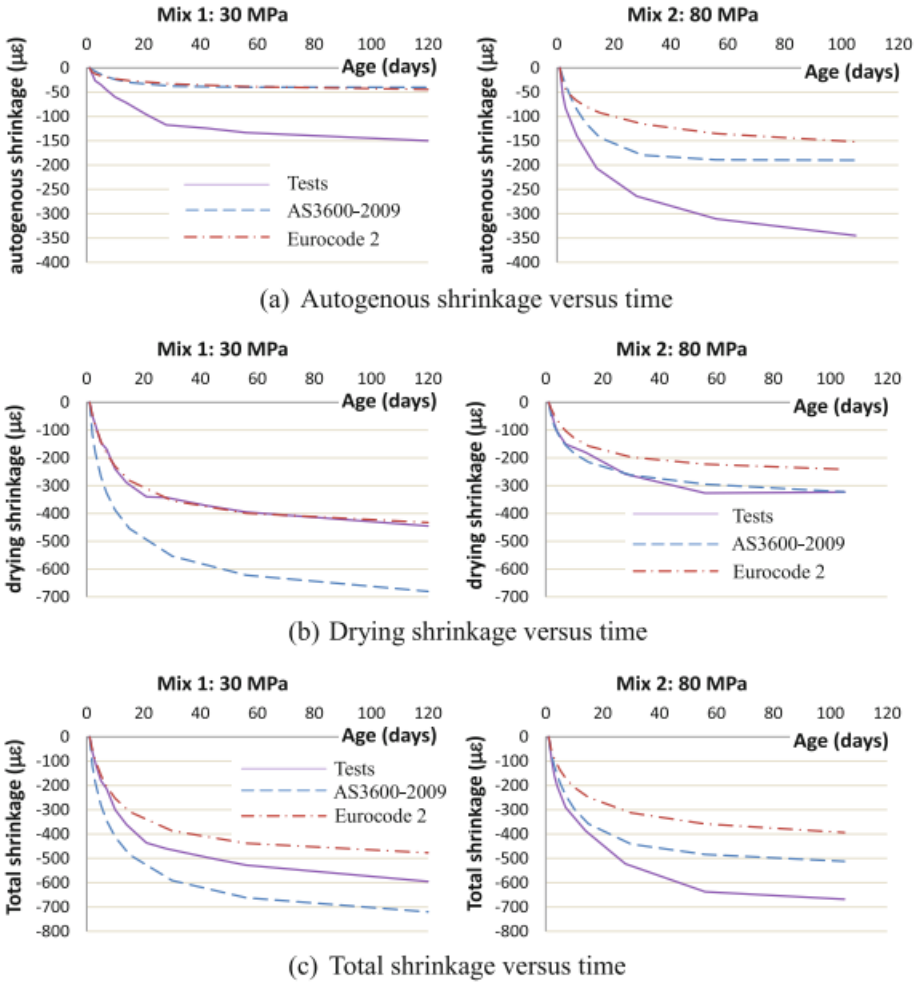

Figure 2. Shrinkage strains comparisons. Source: Gilbert et al. (2018).

As shown in Figure 3, autogenous shrinkage decreases when the water/cement ratio is increased, and most of this shrinkage occurs within the first 24 hours (Holt, 2005).

The most effective method to reduce autogenous shrinkage has proven to be moist curing. However, it is imperative to emphasize that shrinkage may still occur even when concrete is subjected to 100 percent moist curing (Holt, 2005).

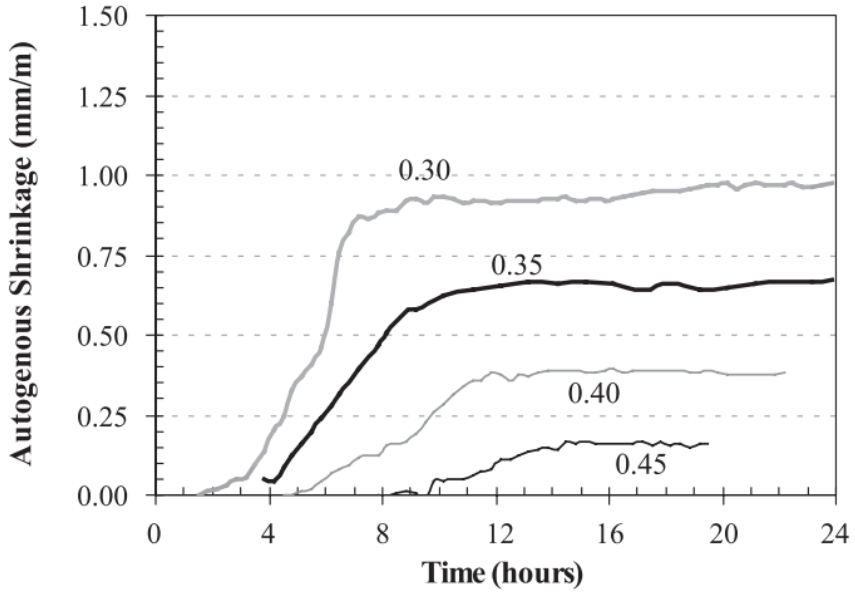

Figure 3. Autogenous shrinkage resulting in changing w/c ratio and equivalent water amount. Source: Holt, 2005.

Currently, there is no standardized procedure to measure autogenous shrinkage. For this reason, many researchers use different measurement techniques that are adapted to the requirements for their experiments (Gilbert et al., 2018; Tang et al., 2021).

2.1.2 Plastic Shrinkage

Plastic shrinkage occurs when fresh concrete loses moisture to reach equilibrium with the environment right after casting and before hardening. This type of shrinkage occurs when the concrete is fresh during the plastic state. Both types of variables that affect this type of shrinkage are concrete composition and environmental conditions like ambient temperature, humidity, and content of cementitious materials (Elzokra et al., 2020).

When the environmental conditions are dry, plastic shrinkage is more likely to develop due to rapid moisture loss and low rate of bleeding during the setting. Plastic shrinkage cracks are usually small but may extend to several feet and can represent a problem on the structure because they can allow the infiltration of external agents into the concrete.

In addition to moisture loss, three more primary factors can induce plastic shrinkage. For reinforced concrete, differential settlement of a restrained section can induce stress. Another factor is thermal differential movement that will be discussed in Section 2.1.5, Thermal Shrinkage. The third factor is autogenous shrinkage. These factors either can act together or independently to increase the probability of cracking (Weiss, 2022).

In 2013, an investigation showed that the addition of synthetic fibers at low volumes effectively reduce the plastic shrinkage cracks (Boshoff & Combrinck, 2013). Coarse fibers are less efficient than finer fibers while reinforcing concrete (Qi et al., 2003). ASTM C1579 proposes a methodology of how to evaluate plastic shrinkage of restrained fiber reinforced concrete. The purpose of this test is to evaluate the effects of evaporation, settlement, and early autogenous shrinkage on the plastic shrinkage cracking performance before setting (ASTM C1579, 2021). Mix composition significantly affects plastic shrinkage. Increasing water-cement ratio increases both bleeding and rate of evaporation (Almusallam et al., 1998).

By understanding plastic shrinkage behavior, it is possible to mitigate the risk of plastic shrinkage cracks. Studies have shown several ways of preventing them, such as reducing the concrete temperature, fog sprays, or placing concrete in the morning (White, 1975).

2.1.3 Drying Shrinkage

Drying shrinkage starts when the concrete is set. The heat that is generated by the exothermic reaction of the cement hydration leads to evaporation of the water, which contributes to what is known as drying shrinkage. The main variables affecting drying shrinkage are mix proportion, construction practices, and environmental conditions (Hasan, 2020). Bridge decks are more susceptible to cracking induced by drying shrinkage because they have a larger surface area to volume ratio (Gribniak et al., 2007).

Coarse aggregates in concrete physically restrain the shrinkage of hydrating and drying cement paste, depending on the ratio between the modulus of elasticity of the aggregate and paste. Larger aggregates can prevent micro cracks due to shrinkage from developing into macro cracks (Karagüler & Yatağan, 2018). Historically, studies have shown that using different kinds of aggregates can have an impact on drying shrinkage in the range of 120 percent to 150 percent (Meininger, 1966; Powers, 1959; Tremper & Spellman, 1963).

The type and duration of curing can affect the rate and ultimate amount of drying shrinkage. Curing compounds, sealers, and coatings can trap free moisture within the concrete for long periods, resulting in delayed shrinkage. Wet curing methods, such as fogging or wet burlap, hold off shrinkage until curing is terminated, after which the concrete dries and shrinks at a normal rate (Kosmatka & Wilson, 2011). Another study showed that when using admixture surface treatments, such as silane-treated carbon fibers, the effects of cement paste's drying shrinkage were reduced by 32 percent (Xu & Chung, 2000). In 2019, a study was conducted to evaluate the alkali activated binders on drying shrinkage compared with normal Portland cement (Matalkah et al., 2019). The results showed that drying shrinkage on alkali activated

binders concrete was about twice that of Type I Portland cement and that the use of some additives can reduce the shrinkage but also reduce the mechanical strength of concrete.

2.1.4 Carbonation Shrinkage

Carbonation shrinkage is a chemical reaction leading the concrete to reorganize its microstructure, pore coarsening, reduced strength cohesion and decrease its porosity (Ye et al., 2017). In this process, concrete absorbs CO_2 in the atmosphere. Carbonation shrinkage is restrained by sand particles, which makes concrete less prone to cracking than mortar (Houst, 1997).

2.1.5 Thermal Shrinkage

Thermal shrinkage results from a decrease in concrete temperature due to the difference between it and the ambient conditions and typically occurs in the first 12 hours (Holt, 2005). There is evidence that time of pouring has relevance on the concrete's strength development, with a higher early strength for concretes poured at higher temperatures that, consequently, may induce early cracking (Sofi et al., 2014).

The effect of the type of aggregate on early-age thermal cracking of concrete has been studied (Chilwesa et al., 2020). This study concluded that the aggregate influences the cracking potential of concrete, where mixes made with basalt and limestone performed better compared with those made with granite. This study also reported that the use of the dual-ring test to assess shrinkage and expansion subjected to various temperatures is very similar to field conditions.

2.2 Effects of Aggregate in Concrete Shrinkage

Coarse and fine aggregates constitute approximately 80 percent of a concrete mixture. Therefore, the aggregate used in concrete can have a significant impact on its workability, durability, cracking behavior, among other properties. Characteristics like shape, size and source of the aggregate are the most important to account for. Aggregate type selection depends on natural resources and industry production. Wyoming aggregate mining operations include granite, limestone, sand and gravel, and scoria (Luhr, 2015). Most common concrete mixtures use granite or limestone fine and coarse aggregates.

Generally, compressive strength of concrete is influenced by the physical and mechanical properties of the aggregate used. It is important to use good quality materials because the

bond between the aggregate and the cement paste depends on the strength, gradation, and stiffness of the aggregate. During the hardening process, thermal characteristics of concrete are dictated by the type of aggregate, which leads to potential early cracking (Klemczak et al., 2017).

There have been studies that show a strong correlation between aggregate type and concrete shrinkage, as aggregate serves as a restraint on the cement paste's shrinkage (Fujiwara, 2008). The main property of the aggregate that affects shrinkage of concrete is drying shrinkage of the aggregate (Hyodo et al., 2013). Elastic modulus and water absorption rate of the aggregate are two other important properties directly related to shrinkage in concrete (Nakamoto et al., 2012).

Coarse aggregates in concrete physically restrain the shrinkage of hydrating and drying cement paste, depending on the ratio between the modulus of elasticity of the aggregate and paste. Larger aggregates can prevent microcracks due to shrinkage from developing into macro cracks (Karagüler & Yatağan, 2018). Historically, studies have shown that using different kinds of aggregates can have an impact on the drying shrinkage in the range of 120 to 150 percent (Meininger, 1966; Powers, 1959; Tremper & Spellman, 1963). Compressive strength of concrete is not directly affected by the aggregate content (Kozul & Darwin, 1997).

Limestone aggregate has been shown to effectively reduce the drying shrinkage strain of concrete with minimal mass loss (Hwang et al., 2021; W. Zhang et al., 2013) while granite can experience significant shrinkage due to its high water absorption and lower modulus of elasticity in comparison with limestone (Aquino et al., 2010; X. Chen et al., 2012; Góra & Piasta, 2022). On the other hand, there are studies that concluded that granite performs better than limestone (W. Chen et al., 2021; Golewski, 2024; Tufail et al., 2017). The dual-ring test has been used to assess the effect of aggregate type on early cracking of concrete subjected to temperature changes (Chilwesa et al., 2020). In this study, concrete made with limestone performed better in comparison with granite specimens, even though both types of aggregates had similar moduli of elasticity. In a numerical study conducted in 2017, cracking behavior was assessed for various aggregate types, results suggested that gravel (consisting mainly of quartz) is the least preferred aggregate, followed by basalt and limestone. Granite showed the best performance in terms of minimizing volume changes (Klemczak et al., 2017). There is a study that has been carried out to compare the effects of limestone and granite on shrinkage and concluded that the aggregate type is not significant on shrinkage (Woyciechowski et al., 2016).

Cement paste and concrete aggregate have different thermal and mechanical properties, and because of these, stresses at a mesoscopic level due to hardening are propagated during the

hardening process. The influence of the aggregate characteristics on the drying shrinkage of mortar and concrete specimens has been studied. In this study, it was found that the coarse aggregate shrinkage strain, specific surface area of aggregate, absorption ratio and pore structure are the main characteristics that affect drying shrinkage (W. Zhang et al., 2013).

Increasing aggregate size helps to decrease shrinkage (Karagüler & Yatağan, 2018). A minimum grain size equal or bigger than 9 mm is recommended. In another study, it was shown that mortar specimens tend to develop higher drying shrinkage compared to concrete. This is because fine aggregate represents less volume portion in a concrete mix in comparison to a mortar mixture (W. Zhang et al., 2013). As the size of the aggregate increases, the ultimate drying shrinkage of the specimen decreases due to the restraining effect of larger aggregates (Gangolu, 2001). The shrinkage of concrete decreases with higher stiffness of the aggregate and greater total aggregate's volume concentration (Tangtermsirikul & Tatong, 2001).

In a study using Finite Element Modeling (FEM) to simulate cracking caused by autogenous volume deformation, the impact of aggregate size on the morphology of the damage zone was determined. Short and wide damage zones tended to form around large aggregates, whereas long and narrow zones tended to form around small ones (G. Zhang et al., 2018). In another numerical investigation, shrinkage cracking in cementitious composites was modeled, revealing that cracking density upon drying increases with aggregate size and volume fraction (Idiart et al., 2012).

Aggregate gradation can significantly influence compressive strength and workability of concrete (Ashraf & Noor, 2011). The quality of the interface between cement paste and the aggregates can result in a reduction up to 70 percent of the original compressive strength (Guinea et al., 2002).

Concrete shrinkage control can be achieved by combining two main factors: reducing water content and ensuring appropriate aggregate characteristics.

2.3 Assessment of Early-Age Cracking

Xi et al. (2003) performed a study to assess cracking in bridge decks that had been recently built in Colorado. The main objective of this study was to clearly identify the causes of cracking and the amount of damage present in the bridge decks. They identified the main variables contributing to cracking, such as shrinkage, temperature changes, mix design, construction process, and environmental conditions. Researchers concluded that these variables should be

accounted for and carefully controlled to minimize cracking. Recommendations to mitigate cracking can be found in the original paper.

Models to predict early-age cracking of concrete bridge decks and slabs have been developed. Bolander (2018) conducted a study where they evaluated the effects of joint spacing, reinforcement detailing, and curing techniques on early-age cracking.

A very well-known method to assess the impact of different variables on the early-age cracking is the single-ring method. In this method, concrete is cast around a steel ring that acts by restraining the concrete movements. Strains are measured at different points of the steel ring to evaluate if a crack has been formed. A full description is available in Section 4.

The dual-ring test is a relatively new method to assess cracking in concrete specimens, but there has been a notable increase in the utilization of this test because of its advantages. These studies demonstrated that the dual ring is a good method to characterize cracking propensity of different types of concrete (De La Varga et al., 2018, 2019; Wilson & Weiss, 2020). This test is modified to obtain the same degree of restraint of the ASTM C1581 (2004) (Schlitter et al., 2010).

2.4 Mitigation Methods

Mitigation methos are used to improve the durability of concrete. In this section, we will discuss different measures to mitigate early-age cracking. The most effective methods include the use of fibers in the mix, admixtures, and internal curing. These methods focus on the properties of the mix itself. Other mitigation methods, such as constructive joints or controlling environmental conditions, are not discussed.

2.4.1 Fibers

When shrinkage is present on an element that is restrained against movement, internal stresses develop. In the early stages of the setting process, concrete has very low strength, both compressive and tensile. However, the tensile strength of concrete is significantly lower. A crack will form whenever internal tensile stresses are superior to concrete's tensile strength. Adding fibers to the mix is a widely used method to provide a higher tensile strength to early-age concrete.

In general, fibers create a bond in the paste between the aggregates. The fibers prevent the cracks from propagating, allowing concrete to behave as a ductile material instead of a brittle material and perform better under tensile stresses.

Fibers are an effective measure to mitigate cracking in concrete regardless of the material they are made of. The effectiveness in controlling cracking depends on the type, diameter, length, and geometry of the fibers. These parameters have been studied for four different types of fibers with different dosage rates where it was concluded that the finer the fiber, the more effective their effect in controlling plastic shrinkage. In a similar way, longer fibers were demonstrated to be more effective than shorter fibers (Banthia & Gupta, 2006). According to Naaman et al. (2005), the most significant parameters in controlling plastic shrinkage cracking during the first 24 hours after mixing are the volume fraction and diameter of fiber reinforcement. The incorporation of fibers into the concrete mixture has been showed to reduce plastic shrinkage cracking by up to 80 percent (Pillar & Repette, 2015).

A summary of the fiber type, dosage, and its effect on the compressive, tensile, and flexural strength is showed in Table 1.

Table 1. Summary of the effects of fibers on the concrete strength.

Fiber type	Length (mm)	Dosage (%)	f_c	f_t	f_r	Study
Polypropylene	12	≥2	↓	↑	↔	(Ahmad et al., 2022)
Steel	13	0-6	↑	-	-	(Pourbaba et al., 2018)
Polypropylene, polyolefin, and steel	12-48	0.2	↔	-	-	(Yousefieh et al., 2017)
Steel, zinc-coated, brass-coated, polypropylene, and polyethylene terephthalate	30-50	2	↑	-	↑	(Corinaldesi & Nardinocchi, 2016)
Steel, polypropylene	30, 50	0.76,1	↔	-	-	(Pillar & Repette, 2015)
Polypropylene	38	0.11, 0.32, and 0.54	↔	↔	↔	(Mendoza et al., 2011)
Polypropylene	6-50	0.6-9	↔	-	-	(Myers et al., 2008)
Polypropylene	19	0.2	↑	↔	-	(Aulia, 2002)
Steel	15	1	↔	↑	↑	(Balendran et al., 2002)
Steel, polypropylene	6-40	0.15-0.9	↔	↔	-	(Qian & Stroeven, 2000)

The evaluation of crack propagation using different types of fibers has been evaluated. From this study, it was demonstrated that monofilament polypropylene fibers are more effective than fibrillated polypropylene in enhancing the mixture for crack growing (Banthia & Nandakumar, 2003). In 2017, Yousefieh et al. evaluated the effectiveness of four different types of fibers and concluded that increasing the modulus of elasticity of the fibers contributes to the mitigation of drying shrinkage.

Polypropylene fibers have a positive impact on early-age shrinkage but may decrease slump (Myers et al., 2008). The addition of fibers into concrete mixtures has been found to decrease workability by reducing the slump values of the fresh concrete mixtures (Latifi et al., 2022; Ramujee, 2013).

On the other hand, the addition of a low volume of fibers (1 percent by volume) has little effect on compressive strength but improves the tensile strength of concrete (Balendran et al., 2002).

Similarly, Ahmad et al. (2022) reported no significant effect on the compressive strength of concrete but an improvement on the tensile strength with the incorporation of polypropylene fibers. In this study, it was also concluded that adding higher doses of fibers (more than 2 percent by volume) can decrease the compressive strength and durability of concrete due to the decrease in the water absorption. For this reason, it is recommended to use an optimal dose between 1 and 2 percent of fibers.

In a study conducted in 2008, the impact of fibers on different parameters was evaluated. It was found that the addition of polymer fibers to the concrete increased the compressive strength at an early age (24 hours), while in the long term, there was no significant impact on the strength (Myers et al., 2008).

In others studies, the addition of fibers showed no considerable effect in the compressive and tensile strength of the concrete (Mendoza et al., 2011; Yousefieh et al., 2017). However, the incorporation of fibers in restrained concrete experiments have several effects on the results: it reduces the crack length and width, it changes the cracking pattern , and deferrers cracking time (Yousefieh et al., 2017).

The combination of fibers with expansive agents (5-10 percent), SRA (1-2 percent), and saturated lightweight sand (10-25 percent) has been studied. The combination of those three mitigation methods with fiber reinforced concrete demonstrated a decrease in the total shrinkage. On the other hand, the addition of these mitigation methods can reduce both compressive and flexural strength properties (Aghaee & Khayat, 2021).

In a different study, researchers evaluated the effect of both fibers and shrinkage-reducing admixtures (SRAs). They concluded that the fibers contributed to controlling the crack size, making them less visible. On the other hand, SRA decreased the overall micro-cracking (Pease et al., 2005; Wei et al., 2024).

In summary, the addition of fibers to the concrete mix is an effective way to mitigate concrete shrinkage cracking. To ensure an effective interaction between the fibers and the concrete, it is very important to account for parameters such as the type, diameter, and volume fraction of fibers in mixes that are more prone to cracking.

2.4.2 Admixtures

Chemical admixtures are added to the mixture to enhance concrete properties. SRAs have a positive impact on the durability of concrete by mitigating shrinkage by delaying the hydration process; but this also leads to a delay in the hardening, which can reduce the compressive strength at early ages (Maia et al., 2012).

SRA molecules work by reducing the polarity of the paste solution, which leads to the hydration retardation of tricalcium silicate and reducing the peak temperature (Kioumarsi et al., 2020; H. Wang et al., 2023; Zhan & He, 2019b). SRAs have shown major changes in the hydration dynamics: a later hydration that leads to a decrease in the maximum temperature of the reaction (Maia et al., 2012).

Several studies have shown that the addition of SRAs to the concrete mix decreased the compressive strength of the concrete up to 20 percent, more remarkably at early ages (Güneyisi et al., 2014; Maia et al., 2012; Oliveira et al., 2014; Yoo et al., 2015). However, other studies that have shown an improvement in the compressive strength of concrete (J.-Y. Wang et al., 2012, 2013).

It has been shown that the addition of SRAs effectively reduces the size of shrinkage cracks (Lura et al., 2007). In 1992, Shh studied the efficiency of shrinkage-reducing admixtures to control restrained shrinkage cracking of concrete. The result of their work shows that SRAs significantly reduce free shrinkage, and there is a considerable reduction in crack width (Shh et al., 1992).

2.4.3 Internal Curing

According to the American Concrete Institute (ACI), internal curing is defined as “a process by which the hydration of cement continues because of the availability of internal water that is not part of the mixing water.” Curing allows concrete to keep enough water during the hydration process where there is an exothermic reaction, which leads to autogenous shrinkage. Concrete mixtures with low water-cement ratio have a limited amount of water to hydrate. Traditional curing methods cannot effectively mitigate this phenomenon. The use of internal curing provides an improvement in hydration, early cracking, and durability of the concrete mixture (Geiker et al., 2004; Şahmaran et al., 2009).

Although lightweight aggregates (LWA) are usually used to reduce concrete’s density, another property that characterizes these types of aggregates is their high capacity of absorption when compared to regular aggregates. Lightweight aggregates are typically used as internal curing materials because it successfully mitigates autogenous shrinkage on concrete mixtures (Bentz & Snyder, 1999; Liu et al., 2017; Shen et al., 2021; Yang et al., 2022; Zhutovsky et al., 2002).

The differences within external and internal curing are illustrated in Figure 4. External curing is when concrete is hydrated by applying water to the surface. The rate of penetration depends on the concrete’s properties, specifically on the absorption. Internal curing allows continued cement hydration by supplying water from pre-wetted aggregates, providing a more uniform distribution of water across the entire section.

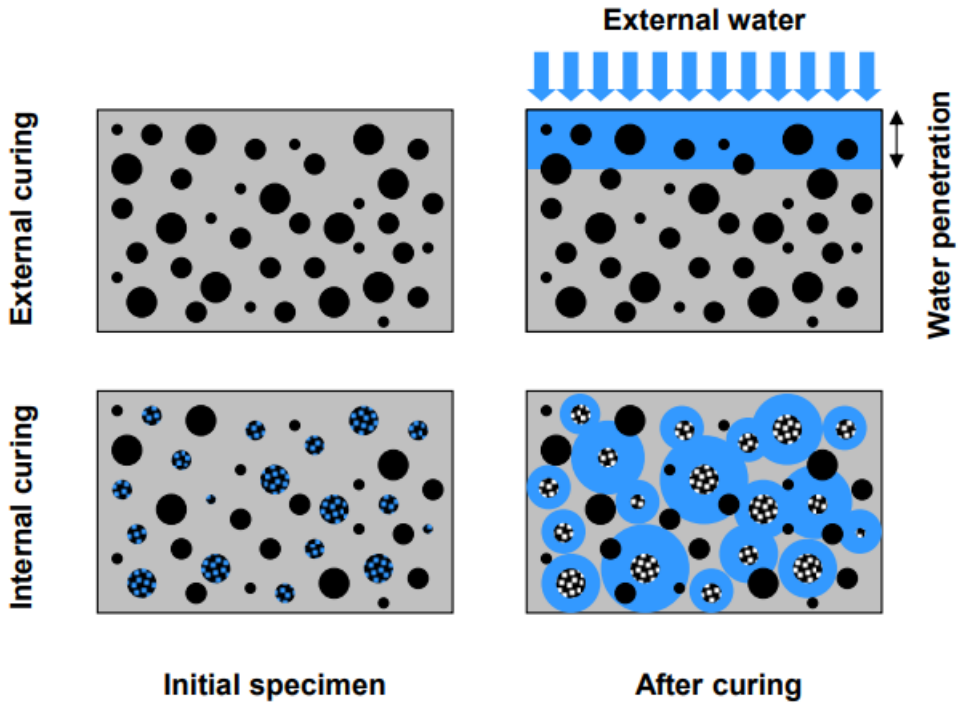

Figure 4. Conceptual illustration of the differences between external and internal curing.

Source: De La Varga et al. (2012).

There are some studies that suggest that the strength of concretes made with lightweight aggregates is enhanced (Kohno et al., 1999). According to Shen et al. (2021), the higher compressive strength was achieved by using 10 to 15 percent of lightweight fine aggregates, and therefore, enhancing concrete's durability as a result of the polymerization degree of C-S-H gels that counteract the negative effects of the porosity of the lightweight fine aggregates. In another study made with concretes with water-cement ratios between 0.30 and 0.35 and a replacement of 4 to 8 percent with lightweight aggregates (LWA), an increase in the compressive strength was observed in all mixtures (Lura et al., 2004).

On the other hand, some researchers have concluded that the compressive strength of concrete is negatively affected by the addition of lightweight aggregates (Takada et al., 1999). For example, a study evaluated the use of lightweight aggregate as partial replacement of 25 percent of the normal-weight aggregate for internal curing and concluded that LWA significantly reduces autogenous shrinkage, but it also has a negative impact on the compressive strength of the concrete (Bentur et al., 2001). Zhutovsky et al. (2004) concluded that if the content of the lightweight aggregates is optimized by replacing a low percentage of the regular aggregates, a small effect on the reduction of the compressive strength will be observed while improving autogenous shrinkage.

The seemingly contradictory results are attributed to differences in LWA properties, mixing ratios, and other factors. In general, coarse lightweight aggregate is used when lightweight concrete is desired. On the other hand, fine LWA is used when internal curing is needed rather than making the whole concrete mix lightweight (Yang et al., 2022).

The addition of lightweight aggregate has a negative effect on the compressive strength during the early stages because it increases the ratio of water to the binder of the mix, but a positive effect is observed in the later stages due to the hydration of cement (Dong et al., 2022). Therefore, the addition of LWA can lead to a decrease of compressive strength but it can be compensated with a prewetting process to meet the required mechanical properties.

In order to prepare a concrete mixture with good mechanical properties while utilizing lightweight aggregates for internal curing and shrinkage reduction, it is essential to take into account physicochemical properties of lightweight aggregates (Shen et al., 2021). The amount of LWFA for internal curing depends on its water absorption and desorption properties. A usage of 0 to 30 percent of LWFA is generally used (Aghaee & Khayat, 2021, 2023; Yang et al., 2021).

2.5 Literature Review Conclusions

From the literature review, shrinkage consists in two major components: drying shrinkage and autogenous shrinkage (Gribniak et al., 2007). Early age shrinkage is most likely attributed to autogenous and thermal shrinkage, depending on the water/cement ratio of the concrete. Autogenous shrinkage decreases by increasing the water/cement ratio. Drying shrinkage is the most significant part of the total shrinkage. The use of fibers, shrinkage reducing admixtures, internal curing materials, and larger aggregates are an effective way to mitigate shrinkage.

3 MATERIALS

3.1 Cement

Type I/II Portland cement meeting the standard ASTM C150/C150M (2024) was used. The cement employed for all concrete mixtures was from a single batch to avoid any effects due to cement variations.

3.2 Aggregates

The first set of specimens was made with granite aggregate obtained with assistance from WYDOT and is labeled GR and the second with limestone aggregate, which is labeled LS. Mechanical properties were determined in accordance with ASTM C127 (2024) and ASTM C128 (2022).

3.2.1 Coarse Aggregates

Aggregates were sieved and modified by selecting the correct weight proportions of the different particle sizes to meet size 67 from ASTM C33 (2024). Granite and limestone properties are shown in Table 2.

Table 2. Coarse aggregate properties. Source: Tanner Research Group.

Type of aggregate	Granite	Limestone
Dry Bulk Specific Gravity	2.53	2.67
Absorption	0.64%	0.45%
Bulk Density	102.62 lb/ft^3 [1643.8 kg/m^3]	100.97 lb/ft^3 [1617.38 kg/m^3]

3.2.2 Fine Aggregates

The fine aggregate was selected to meet ASTM C33 (2024). Its properties are shown in Table 3.

Table 3. Fine aggregate properties. Source: Tanner Research Group.

Type of aggregate	Granite	Limestone
Dry Bulk Specific Gravity	2.65	2.85
Absorption	1.63%	0.17%
Bulk Density	114.73 lb/ft^3 [1837.8 kg/m^3]	111.5 lb/ft^3 [1786.06 kg/m^3]

3.2.3 Lightweight Aggregates

Lightweight aggregate properties were determined according to ASTM C1761 (2023) and are specified in Table 4.

Table 4. Internal curing properties of lightweight aggregate. Source: Arcosa Lightweight.

LWA Absorption	19.2%
LWA Desorption	86.1%
LWA PSD Specific Gravity	1.950

3.3 Fibers

The fibers used in this work were 1.5-inch blended copolymer macro synthetic fibers (Figure 5) complying with ASTM C1116/C1116M (2023). The manufacturer's minimum content is three pounds per cubic yard. The maximum recommended fiber content, eight pounds per cubic yard (4.75 kg/m^3), was used.

Figure 5. Copolymer macro synthetic fibers. Source: Tanner Research Group.

3.4 Admixtures

Shrinkage reducing admixture (SRA) is an admixture specifically formulated to reduce drying shrinkage in concrete. In this work, EUCON SRA-XT, meeting the requirements of ASTM C494 (2024), was used. The maximum recommended dosage of 2 percent by weight of cementitious materials was used on this work.

3.5 Mixture Properties

A total of 16 mixtures were tested in this study. The mix proportions are summarized in Table 5. All mixtures were designed with a 0.45 w/c ratio and a target strength of 27.6 MPa (4000 psi). For the fiber mitigated mixtures, the maximum recommended dosage of 0.2 percent by weight (8 lb/yd^3) was used. For mixtures using SRA, a dosage of 2 percent of cementitious material was used and the water was adjusted to maintain the same water-cement ratio. For mixtures with internal curing, 30 percent of the total weight of the fine aggregate (FA) was replaced by LWFA in saturated surface-dry (SSD) condition. Coarse aggregate (CA) was not replaced by any lightweight material.

Table 5. Test matrix with variables for all experiments. Source: Tanner Research Group.

Mix	Mix proportions (kg/m^3)							
	w/c Ratio	Cement	Water	FA	CA	LWFA	Fiber	SRA
GR – Control	0.45	448.22	201.70	545.70	1233.40	0.00	0.00	0.00
GR – Fiber (F8)	0.45	448.22	201.70	545.70	1233.40	0.00	4.75	0.00
GR – SRA (S2)	0.45	448.22	193.74	545.70	1233.40	0.00	0.00	7.96
GR – Fiber and SRA (F8-S2)	0.45	448.22	193.74	545.70	1233.40	0.00	4.75	7.96
LS – Control	0.45	448.22	201.70	742.20	1027.50	0.00	0.00	0.00
LS – Fiber (F8)	0.45	448.22	201.70	742.20	1027.50	0.00	4.75	0.00
LS – SRA	0.45	448.22	193.74	742.20	1027.50	0.00	0.00	7.96
LS – Fiber and SRA	0.45	448.22	193.74	742.20	1027.50	0.00	4.75	7.96
LW – GR – Control	0.45	448.22	201.70	382.00	1233.40	163.70	0.00	0.00
LW – GR – Fiber	0.45	448.22	201.70	382.00	1233.40	163.70	4.75	0.00
LW – GR – SRA	0.45	448.22	193.74	382.00	1233.40	163.70	0.00	7.96
LW – GR – Fiber and SRA	0.45	448.22	193.74	382.00	1233.40	163.70	4.75	7.96
LW – LS – Control	0.45	448.22	201.70	519.54	1027.50	222.66	0.00	0.00
LW – LS – Fiber	0.45	448.22	201.70	519.54	1027.50	222.66	4.75	0.00
LW – LS – SRA	0.45	448.22	193.74	519.54	1027.50	222.66	0.00	7.96
LW – LS – Fiber and SRA	0.45	448.22	193.74	519.54	1027.50	222.66	4.75	7.96

4 TEST METHODS

4.1 Single-Ring Setup

AASHTO T334-08 (2020) estimates the time to cracking of restrained concrete specimens (Figure 7). The procedure consists of a concrete sample in a circular mold around a steel ring instrumented with strain gages (Figure 8) and determines the effects of variations in the properties of restrained concrete measured as the time of cracking.

Figure 6. Single ring test. Source: Tanner Research Group.

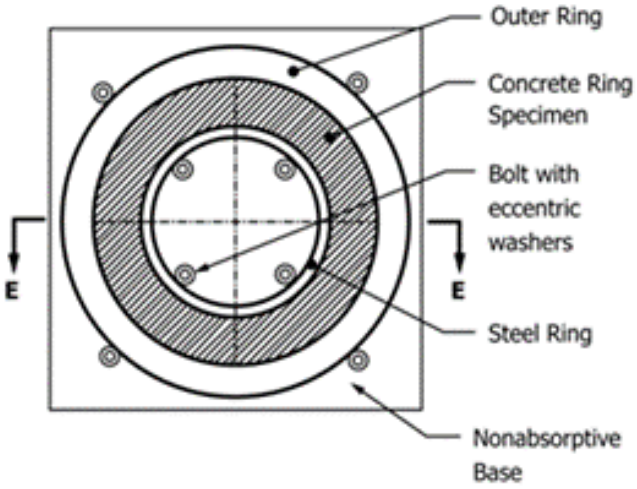

Figure 7. Plan view of the single-ring test. Source: ASTM C1581.

Several single-ring molds were built to the dimensions specified in AASHTO T334-08 (2020), as shown in Figure 9. The molds consisted of a 20 x 20 in. (508 x 508 mm) plywood base with a

plywood ring having an inner diameter of 18 ¼ in. (463.5 mm) attached to it to hold a six-inch strip of ⅛ in. (3.2 mm) thick high-density polyethylene (HDPE) to act as the outer mold. An identical plywood ring was placed on top of wooden spacer blocks at the top of the HDPE strip to provide rigidity during concrete placement, as seen in Figure 10. A six-inch-high (152 mm) steel ring with an inner diameter of 11 in. (280 mm) and an outer diameter of 12 in. (305 mm) was held to an inner circle of plywood by four wooden blocks equally spaced between the four strain gages on the interior of the ring. A polyethylene film was placed on the base plywood sheet to allow the specimen to move laterally.

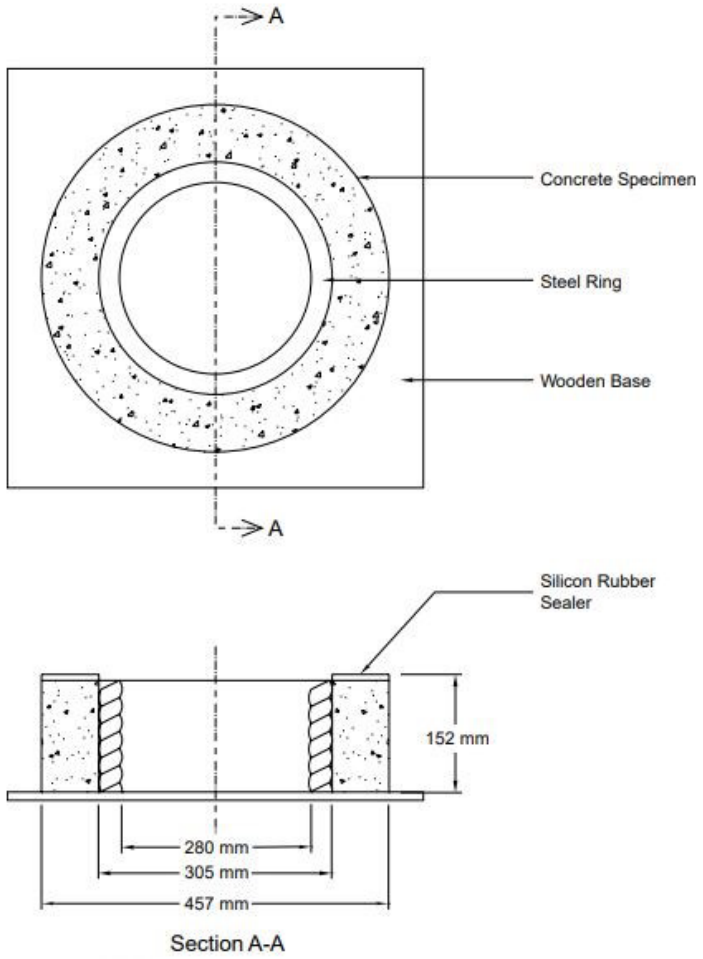

Figure 8. Single-ring specimen dimensions (not to scale). Source: (AASHTO T334-08, 2020).

Figure 9. Single-ring setup. Source: Tanner Research Group.

4.1.1 Instrumentation

The inside of the steel ring was sanded at specific locations to provide a smooth surface. A total of four 5-mm strain gages were placed at quarter points around the inside of the steel rings at mid-height. The strain gages were connected to the University of Wyoming's data acquisition system. Data was recorded every five minutes for the first 24 hours, and every 30 minutes onwards.

4.1.2 Casting Procedures

The concrete was mixed in accordance with ASTM C305 (2020). It was poured in three lifts, and 75 strikes were provided for each lift using a proper steel rod. The concrete was finished with a steel hand trowel and a float with a final view as shown in Figure 10. Approximately one hour after the specimens were poured, wet burlap was placed on top to promote curing. After 24 hours, the exterior HDPE molds were removed, and a plastic cover was affixed to the top of the rings using a silicone caulk to prevent moisture loss. The plywood base was lightly tapped with a mallet to break the rings free from the nonstick plastic on the base, but the specimens were left on their bases to prevent moisture loss through the bottom of the specimens. A single-ring specimen after the removal of the HDPE mold and plastic cover is shown in Figure 7. Note that some silicone caulk is still adhered to the specimen in the picture. Compressive strength was determined after 28 days of casting by testing concrete cylinders (ASTM C39, 2024).

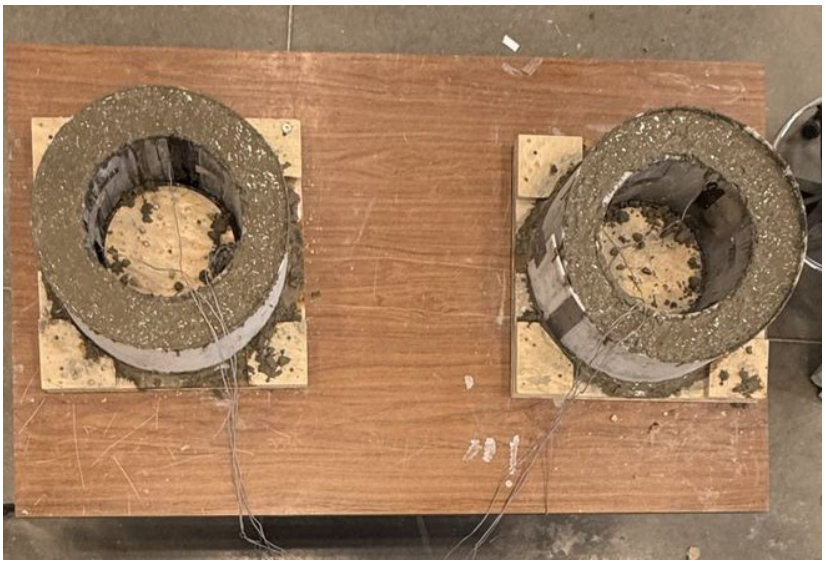

Figure 10. Freshly cast single-ring setup.

4.2 Dual-Ring Setup

Dual-ring shrinkage tests evaluate stress development and cracking potential due to restrained volume change. In this test, temperature and volume changes are controlled with strain gages placed at four equidistant quarter points on both the interior of the inner ring and the exterior of the outer ring (AASHTO T363, 2017) along with thermocouples. This test uses two rings made of a low thermal expansion iron-nickel alloy (Invar) that permits measuring both shrinkage and expansion (Figure 11).

Figure 11. Dual-ring test setup. Source: Tanner Research Group.

Two testing apparatuses were built in accordance with AASHTO T363, 2017 to evaluate the early-age shrinkage behavior. To minimize the effects of temperature variation on the experiment, the rings were fabricated from low thermal-expansion iron-nickel alloy (Invar) with a thermal expansion coefficient of 1.3x10-6/°C, as specified in ASTM F1684 (2021). The low coefficient of thermal expansion of the rings reduces the degree of restraint of the sample during a temperature change (Raoufi et al., 2011). A lower coefficient of thermal expansion of Invar rings will allow temperatures to vary while the rings remain volumetrically stable. The dual-ring test setups were made following AASHTO T363 (2017). Dimensions of the rings are illustrated in Figure 12.

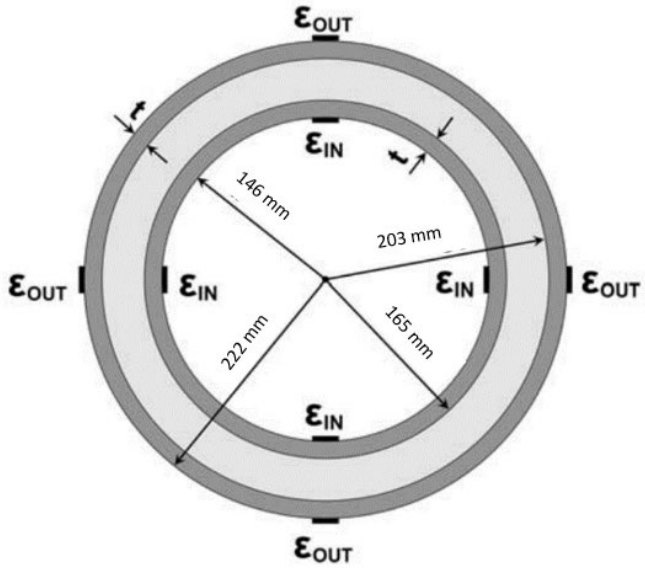

Figure 12. Geometry of dual-ring test. Source: AASHTO T363, 2017.

4.2.1 Instrumentation

In this method, strain was measured in both the inner and outer rings. A total of eight 5-mm strain gages were placed at mid-height in the positions as presented in Figure 12. It is worth noting that the rings are made of invar alloy, for which the proper Micro-Measurements CEA-00-125-UNA-350 strain gages were used.

Prior to adhering the strain gages, each area was previously sanded to reach a mirror-like surface and meticulously cleaned. Strain gages were placed and covered with tape to protect them. In this case the data acquisition system was set to record data every 15 minutes starting to record approximately 10 minutes after casting.

Four thermocouples were positioned at the mid-height of the Invar rings, with two placed on the inner ring and two on the outer ring. Thermocouples were located on the outside of the outer ring and the inside of the inner ring.

4.2.2 Temperature Control System

After four days, an external cooling system was used to induce cracking. The temperature control system consisted of an Anova A40 water bath system pumping ethylene glycol at 15 L/min through a looped copper coil (Figure 13). To distribute the temperature along the concrete ring, a 1/8 in. aluminum plate was placed on the top of the concrete, making contact with both the copper coil and the concrete.

Figure 13. Temperature control system. Source: Tanner Research Group.

4.2.3 Insulating Chamber

The double-ring system was placed in an insulating chamber made of plywood and extruded polystyrene insulation, as shown in Figure 14, to maintain the temperature during cooling. To reduce the friction between the concrete and the plywood, a nonstick plastic sheet was attached between them. With this insulation system, the lower temperature limit of the equipment was achieved when the water bath reached a temperature of -30°C (-22°F) and the concrete inside the Invar rings was at -5°C (23°F).

Figure 14. Insulating chamber. Source: Tanner Research Group.

4.2.4 Temperature Correction

When using bonded strain gages, the measured strain should exclusively reflect the material response during testing and remain unaffected by other environmental variables. However, because strain gages work by electrical resistance, they also respond to external temperature changes.

When an experiment experiences a range of temperatures, results from strain gages can vary due to the resistance change in the gage caused by temperature and being independent of mechanical strain. Additionally, the gage factor, which is the relationship between strain and resistance change, can also vary with temperature changes. This potential source of error can be the most significant in restrained tests (Micro-Measurements, 2014) but, when is fully understood and addressed, can be compensated, or corrected.

Thermal output is proportional to the change in resistance of the gage installed on a stress-free specimen subjected to temperature variations. It is due to two main factors: the electrical resistivity of the grid alloy of the gage and the differential thermal expansion between the grid conductor and the material under test to which it is bonded (Micro-Measurements, 2014). The total change in the resistance can be expressed by Equation 1.

$$\frac{\Delta R}{R} = [\beta_G + (\alpha_s + \alpha_G)F_G]\Delta T$$

Equation 1. Total change in the resistance of a strain gage under a temperature change. Source: (Micro-Measurements, 2014).

Where:
ΔR/R = Unit resistance change.
β_G = Thermal coefficient of resistivity of grid material.
α_s = Thermal expansion coefficient of the ring material and specimen.
α_G = Thermal expansion coefficient of the grid within strain gage.
FG = Gage factor of the strain gage.
ΔT = Temperature changes from arbitrary initial reference temperature.

It is important to take this effect into consideration because the gages themselves are going to experience strain due to temperature variation. There are three basic methods of compensation available: the simultaneous recording of strain and temperature, temperature-compensating circuits, and self-temperature compensation (STC) (Hannah & Reed, 1992).

STC has been successfully used for the dual-ring experiment by using a datalogger from National Instruments and LabView software (Chilwesa et al., 2020). However, the authors combined STC with the response of each gage to temperature variation to account for the difference between the grid and the invar thermal expansion.

There are several factors that may affect the thermal output of a strain gage such as shape of the tested specimen, grid alloy and lot or package of the strain gage, bonding materials, and installation procedures. Because of this reason, it is the best practice to evaluate each gage under the expected thermal ranges for the experiment (Micro-Measurements, 2014).

For this project, CEA-00-125UNA-350 strain gages were used with constantan (a copper-nickel alloy) grid designed for temperature ranges of –100° to +350°F [–75° to +175°C]. These gages were corrected using Equation 2 and Equation 3, which takes into consideration all the previously mentioned variables.

$$\mu\varepsilon = -145 + 4.06T - 3.39x10^{-2}T^2 + 8.29x10^{-5}T^3 - 6.68x10^{-8}T^4$$

Equation 2. Temperature correction equation. Source: Micro-Measurements lot information.

Where T is temperature in °F;

$$\mu\varepsilon = -47 + 3.85T - 8.54x10^{-2}T^2 + 4.34x10^{-4}T^3 - 7.01x10^{-7}T^4$$

Equation 3. Temperature correction equation. Source: Micro-Measurements lot information.

Where T is temperature in °C.

For the temperature range of 20° to 80°F [–7° to +27°C] used in this project, thermal output varies from -80με to 3με approximately as shown in Figure 15.

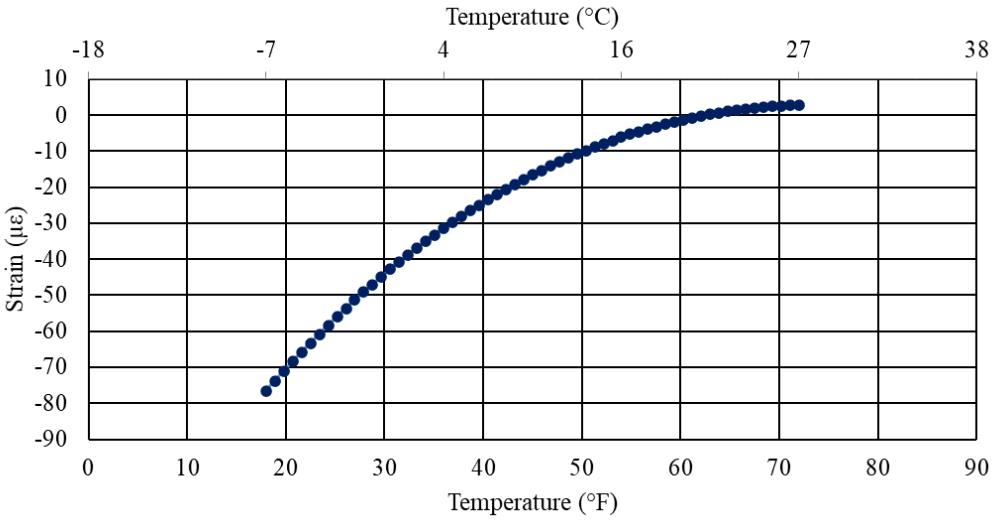

Figure 15. Thermal output of Micro Measurements gages. Source: Tanner Research Group.

Another method to correct thermal output of each gage is the firsthand corrective measurement. In this method, a thermal output for each gage under the temperature ranges in the unstressed rings is generated by simulating the experiment without a concrete ring inside the invar rings (Schlitter et al., 2010). This method directly considers the shape of the specimen, strain gage material, bonding materials, and installation procedure.

An example of the firsthand corrective measurement for one strain gage attached to an invar ring in a dual-ring setup is illustrated in Figure 16 where it is observed that for the temperature range of 20° to 80°F [–7° to +27°C], thermal output varies from -420με to 15με. The difference of strains between Equation 2 and the thermal output of one gage indicates that there are other specific factors that can affect the thermal output without a specimen, as mentioned above.

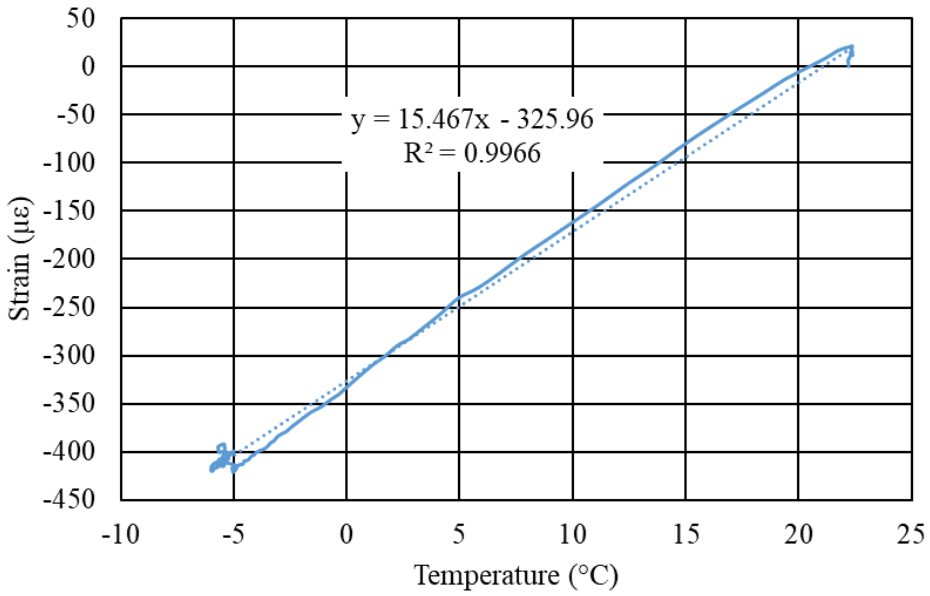

Figure 16. Thermal output of one gage. Source: Tanner Research Group.

4.2.5 Casting Procedures

The dual-ring specimens were placed in two lifts and rodded 75 times per lift to ensure good consolidation. The specimens were then finished by hand with a float and a trowel to achieve a relatively flat surface Figure 16. For each batch of concrete, a minimum of nine 4 x 8-inch (100 x 200 mm) concrete cylinders were made to test mechanical properties.

For internal cured specimens, the lightweight fine aggregate (LWFA) was pre-saturated for 72 hours. Then the LWFA was let sit for about 4 hours until SSD condition was reached. The cone test (ASTM C128, 2022) was used to determine if the LWFA reached the SSD condition.

Figure 17. Freshly cast dual ring setup. Source: Tanner research group.

4.2.6 Cracking time

For the dual ring, strain measurements were recorded every 5 minutes and tabulated for each of the eight strain gages. A crack was considered to have occurred when a difference in strain was greater than 20 microstrain between two consecutive readings.

5 RESULTS AND DISCUSSIONS

5.1 Age at Cracking

Measurements from individual strain gages were recorded at 5-min intervals from the finish of casting until the end of testing. Cracking time was recorded when an instantaneous strain decrease of more than 30 or 20 microstrain occurred in one or more gages, in the single- and dual-ring tests, respectively. A minimum of two specimens were made from each batch, and the average cracking time is represented in the results.

For granite mixtures (Figure 18), the results are consistent with the existing literature, confirming that the incorporation of fibers, SRA, LWFA, or a combination of these materials significantly delays cracking in concrete. Specifically, the results align with (Latifi et al., 2022), which demonstrated that crack resistance is improved with the addition of fibers. The addition of fibers performed similarly to SRA mitigated mixtures. Among the mitigation methods employed in this work, the replacement of 30 percent fine aggregate with lightweight fine aggregate proved to be the best single measure for both types of experiment.

Additionally, when two mitigation measures are combined, the addition of fibers in combination with SRA showed the best performance. The combination of the three mitigation methods has the best overall performance showing no cracking during the whole duration of experiment due to their synergistic effect. SRA improves the pore structure of the concrete, decreasing capillary stress and reducing evaporation of water while the internal curing releases water to replace the amount of water that is evaporated. Additionally, fibers act as a reinforcement that make concrete more ductile .

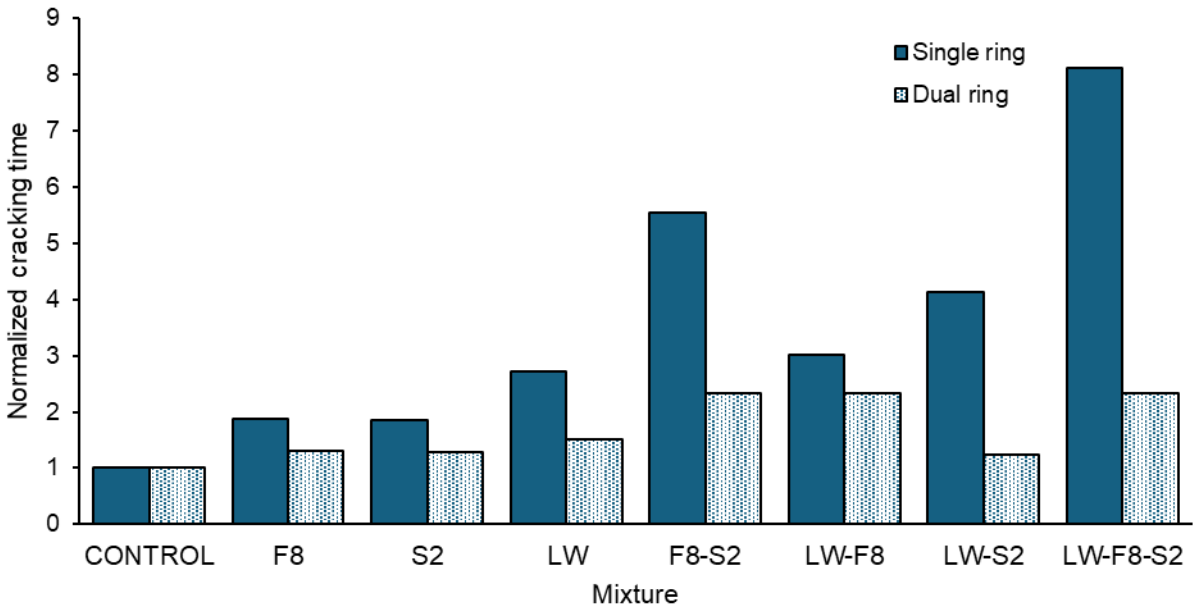

Figure 18. Granite specimens normalized cracking time.

For mixtures made with limestone (Figure 19), the addition of SRA resulted in the best performance as a single mitigation measure. When combining two mitigation measures, internal curing with fibers proved to be the most effective. Overall, SRA was the best performing mitigation measure; however, it is important to point out that internal curing had a superior performance in comparison with other mitigation measures.

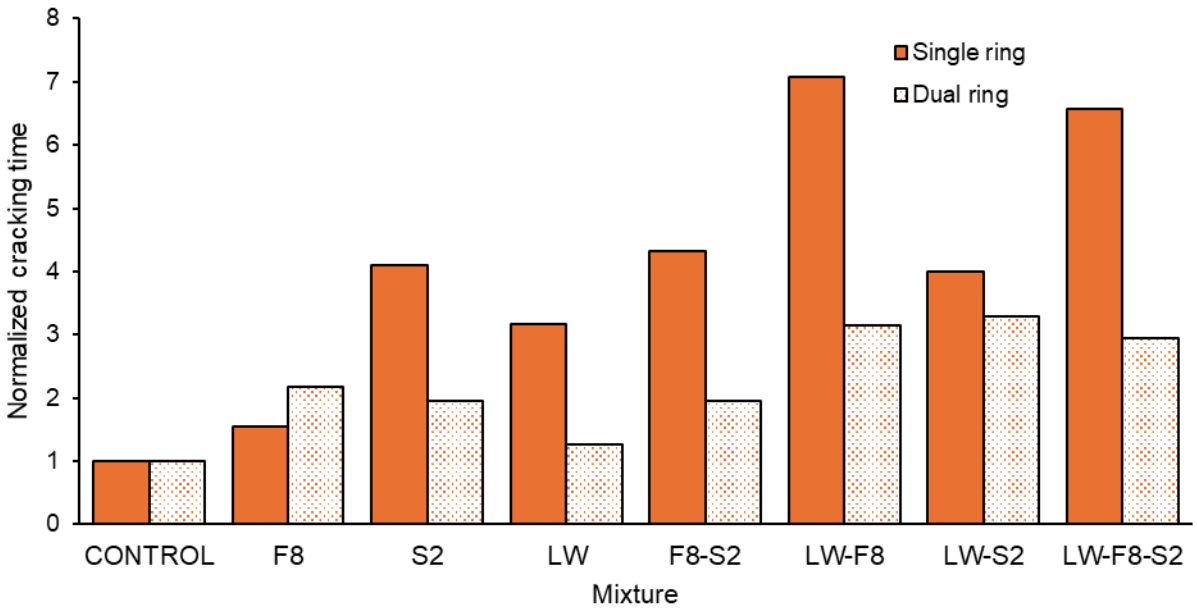

Figure 19. Limestone specimens normalized cracking time.

Figure 20 and Figure 21 show the average normalized cracking time of single- and double-mitigated mixtures using the single ring and the dual ring, respectively. Both control mixtures cracked at 24 hours, but limestone performed notably better compared to granite mixtures. In the single-ring test, the cracking time of limestone mixtures was up to five times the original, while granite mixtures were up to 4 times the original. It is also notable that double-mitigated mixtures generally performed better than single-mitigated ones.

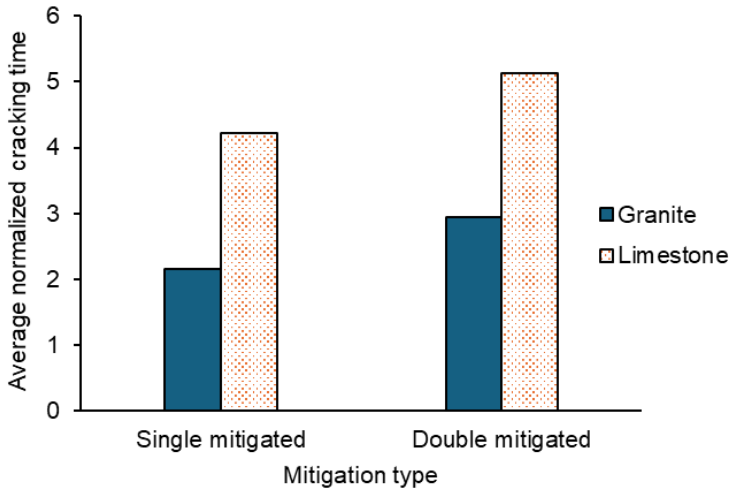

Figure 20. Average normalized cracking time of single-ring experiments.

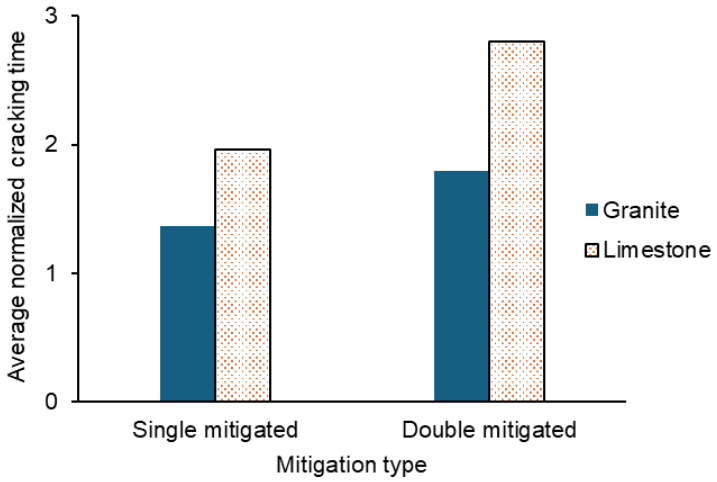

Figure 21. Average normalized cracking time of dual-ring experiments.

The average normalized cracking time of all specimens is presented in Figure 22. Single-ring results showed a greater normalized cracking time compared to the dual-ring results. For granite mixtures, the average normalized cracking time was 4, while for the dual ring, it was less than 2. For limestone mixtures, the values were 5 for the single ring and 2.4 for the dual ring. Although both experiments showed the same tendency, the dual-ring average cracking time is half of the single-ring results. This is because cooling was applied at 4 days, thus inducing cracking. On the other hand, the single-ring test demonstrated greater consistency in measuring cracking time with lower overall coefficient of variation when averaging results across all variables.

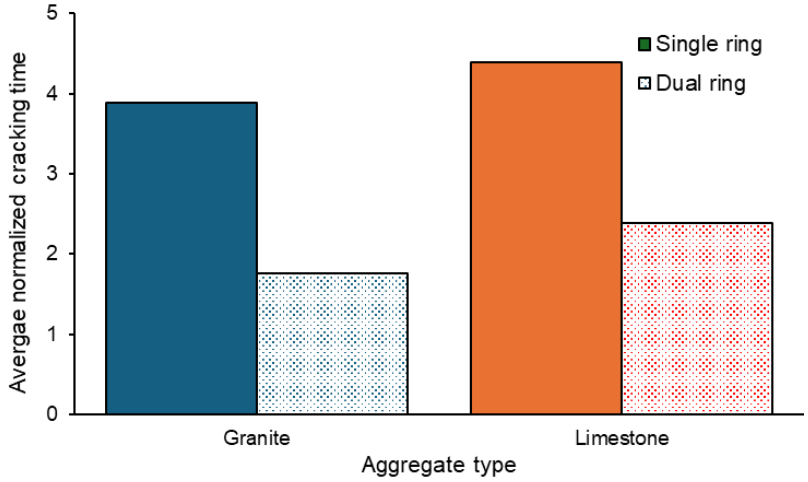

Figure 22. Comparison between dual- and single-ring tests.

5.2 Mechanical Properties

Compressive strength results of each mixture are reported in Table 7. A minimum of 3 cylinders were tested and results did not differ more than 7 percent according to ASTM C39 (2023) for laboratory conditions. Splitting tensile results are also reported in Table 7 with a coefficient of variation not greater than 14 percent (ASTM C496, 2017).

Table 6. Compressive and tensile strength results. Source: Tanner Research Group.

Mixture	Aggregate type	Compressive strength (MPa)	Control comparison (%)	Tensile strength (MPa)	$\frac{Tensile\ strength}{Compressive\ strength}$ (%)
Control	Granite	30.10	100%	3.30	11%
F	Granite	31.66	105%	3.49	11%
SRA	Granite	21.85	73%	3.18	15%
F+SRA	Granite	24.34	81%	3.32	14%
LW	Granite	36.05	120%	3.48	10%
LW+F	Granite	37.43	124%	3.94	11%
LW+SRA	Granite	38.21	127%	4.25	11%
LW+F+SRA	Granite	36.37	121%	4.01	11%
Control	Limestone	30.69	100%	2.84	9%
F	Limestone	29.75	97%	3.49	12%
SRA	Limestone	26.04	85%	3.33	13%
F+SRA	Limestone	27.88	91%	3.51	13%
LW	Limestone	36.85	120%	4.62	13%
LW+F	Limestone	34.02	111%	4.15	12%
LW+SRA	Limestone	28.74	94%	2.51	9%
LW+F+SRA	Limestone	28.46	93%	3.30	12%

Results of granite mixtures suggest that the addition of SRA reduces the compressive strength. It is also observed that the addition of fibers has a positive impact on strength (Abousnina et al., 2021), improving it by 5 percent, and it compensates for the strength reduction caused by SRA when both mitigation methods are combined in the mix because SRA may reduce the compressive strength (Aghaee & Khayat, 2021; Wei et al., 2024). All mixtures with internal curing performed significantly better than the control mixture, with at least a 20 percent increase in strength. There is no significant difference in the percentage of improvement when combining internal curing with other mitigation measures, suggesting that the most efficient mitigation method is the single incorporation of internal curing, which also showed greater consistency than the other mixes. The tensile strength of granite mixtures resulted in an average of 12 percent of the compressive strength. While SRA decreased the compressive strength, there was no effect in the tensile strength, which helps to delay cracking time. For limestone mixtures, the behavior was like that of granite. Incorporation of SRA decreased the compressive strength by 15 percent; however, this effect was partially mitigated by the addition of fibers, reducing the strength loss to 9 percent. Internal curing proved to be the most

effective single mitigation method in terms of strength, improving it by 20 percent. When combining internal curing with other mitigation methods, there was no significant difference in strength. The tendency of all results is illustrated in Figure 5 and 6.

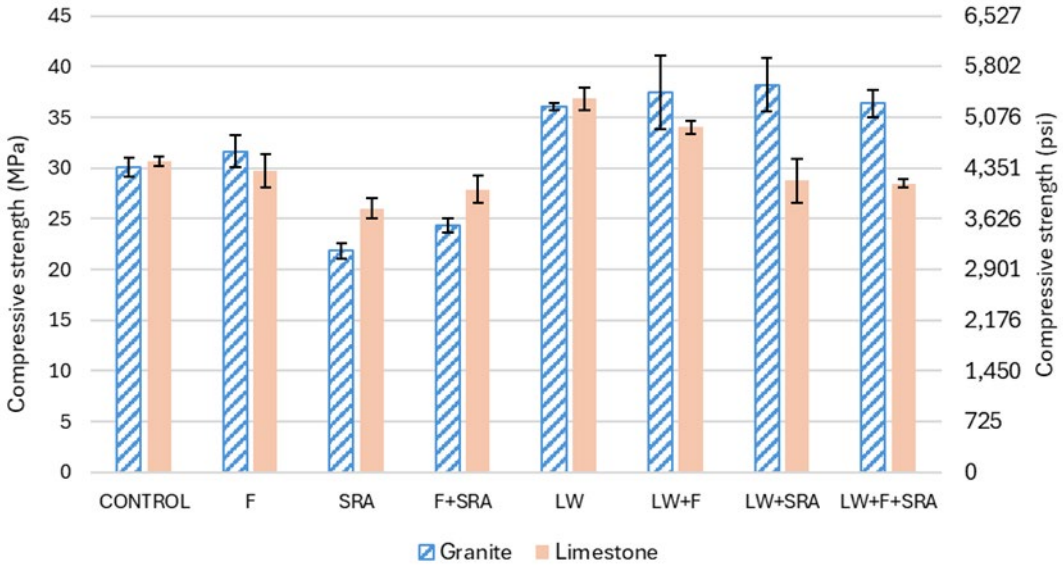

Figure 23. Compressive strength of granite and limestone mixtures. Source: Tanner Research Group.

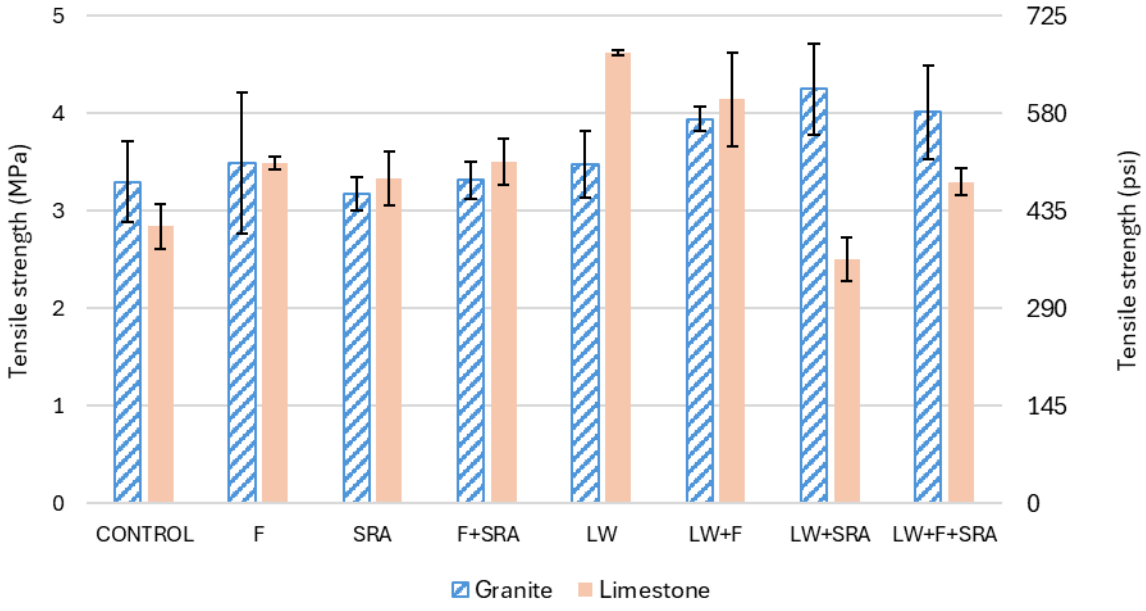

Figure 24. Tensile strength of granite and limestone mixtures. Source: Tanner Research Group.

5.3 Statistical analysis

The objective of this analysis was to evaluate the impact of various mix design parameters on the cracking time of concrete. Specifically, the study considered the effects of Shrinkage Reducing Admixtures (SRA), Fibers, Internal Curing (IC), and Aggregate type (limestone vs. granite). The suite of results from the single ring tests and dual ring tests were considered two separate datasets. This was decided since the two tests are essentially different in setup and the cracking time showed to be generally higher for the dual ring.

5.3.1 Preliminary statistical concepts

The occurrence of random variables can be described through probability distributions such as the widely used normal (gaussian) distribution (Figure 25). When the distribution is used to describe a continuous variable, it is called a probability density function (PDF). Figure 25 shows an example of a normal distribution describing the probability density of the cracking time (C_t) with a mean value defined as μ and standard deviation σ. For PDF's, the area under the curve in between two value points a and b, is equal to the probability of the variable C_t being between those values $P(\alpha \leq C_t \leq b)$. Similarly, the probability of the variable C_t being greater than a certain value point c, $P(C_t \geq c)$ is equal to the area under the right tail of the distribution (Figure 25). It is worth noting that any normal distribution can be transformed into a standard normal distribution, which is a normal distribution with a mean of 0 and standard deviation of 1.

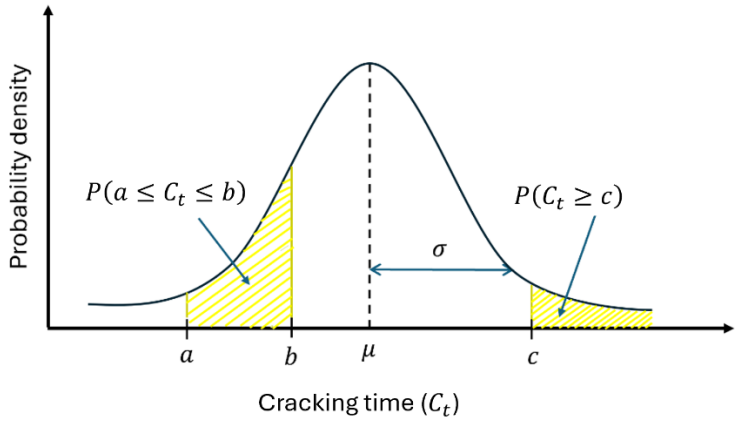

Figure 25. Normal probability distribution for cracking time

When it is desired to compare a sample average with a specific value, a t-statistic is used. The equation for the t-statistic is given by Eq. (1), where $\bar{X}$ is the sample average, *S,* is the sample standard deviation, μ, is the true population average, and *n* is the sample size. In statistical notation, the capital T is the random variable, and a lower-case t refers to the value of the observed data.

(1)

$$T = \frac{\bar{X} - \mu}{S/\sqrt{n}}$$

This statistic follows the Student's t-distribution (Figure 26). In the definition of the pdf for the t distribution, there is a parameter called statistical degrees of freedom (denoted St-DOFs), this can be thought of as the available data points to define the value of the statistic. The value of the statistical degrees of freedom (St-DOFs) is one unit less than the sample size (*n-1*). As the statistical degrees of freedom (or the sample size) increases, the t distribution approaches a standard normal distribution. It is good practice to report the t-statistic with its degrees of freedom as T(St-DOFs)=a. This way, any reader can verify the statistical analysis.

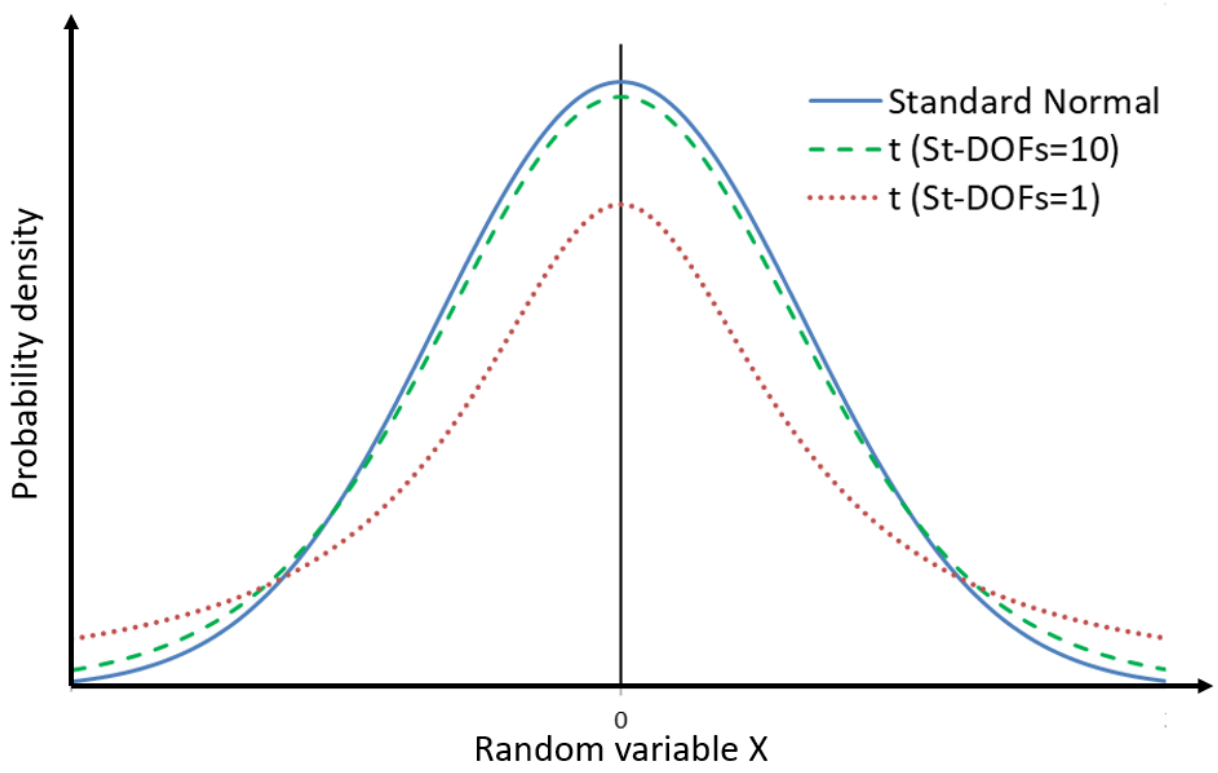

Figure 26. Student's t distribution with different degrees of freedom

Under the classical Null Hypothesis Significance Testing (NHST) the sample average (through the t-statistic) is used to make inferences about the true population average. A null hypothesis is proposed ($\mu = \mu_0$) and this is assumed to be true. This defines a specific distribution. An observed value of the t-statistic can be calculated from sample data and the assumption of the null hypothesis. Then, the probability of obtaining a value of the t-statistic equal or more extreme than the one observed is calculated from the area under the distribution (Figure 27), this value is known as the p-value or observed significance level. It is important to emphasize that this assumes that the null hypothesis is true.

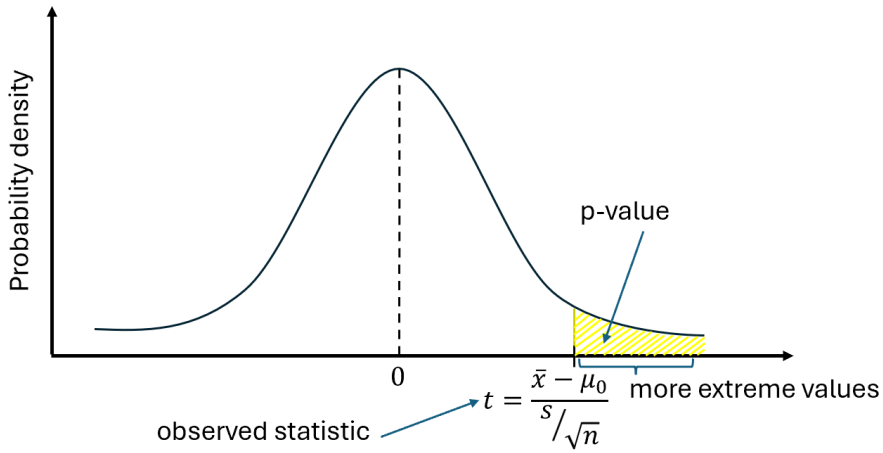

Figure 27. Definition of the p-value

If this probability (p-value) is less than the significance value α (typically α=0.05), this means that the null hypothesis should be rejected (very low probability of observing the data if the null was true). On the other hand, if p-value > α, this means that the null hypothesis cannot be rejected (there is a considerable probability of observing the data if the null hypothesis was true). This process is called a one sample t-test.

There are two choices when comparing sample averages. First, if the two samples are independent, we use an independent samples t-test. Second, if the two samples are not independent, a paired t-test is a better fit. In this type of test, the difference between corresponding data points is calculated and the regular one sample t-test is performed on this difference. The null hypothesis in this case is μ = 0. This means that if the p-value is low enough (<0.05), the null hypothesis is rejected (μ ≠ 0) and this is taken as evidence that the average difference in the samples is statistically significant.

Finally, when more than two laboratory groups are present in a study, an analysis of variance (ANOVA) is the appropriate tool to use. This is also an NHST test where the population variance is estimated in two ways. In broad terms, the method calculates the variance of the means (variability between groups $MS_{between}$) and the mean of the variances (variability within groups MS_{within}). The ratio of these two estimates of the variance is called an F-statistic. The F-statistic follows a Fisher's F distribution (Figure 29). This distribution has two parameters named degrees of freedom (df1 and df2). The first degree of freedom is the total sample size minus the number of groups ($N - a$), and the second degree of freedom is the number of groups minus one (α - *1*). Again, it is good practice to report the F-statistic with its statistical degrees of freedom as F(df1, df2)=c. Finally, a p-value is drawn from the area under the F distribution. As

usual, a p-value is the probability of finding a value of the statistic equal or more extreme than the one observed. If the p-value is below the significance level (α=0.05), the null hypothesis is rejected. For the case of ANOVA, the null hypothesis states that the mean of all groups is the same, or that they come from the same population.

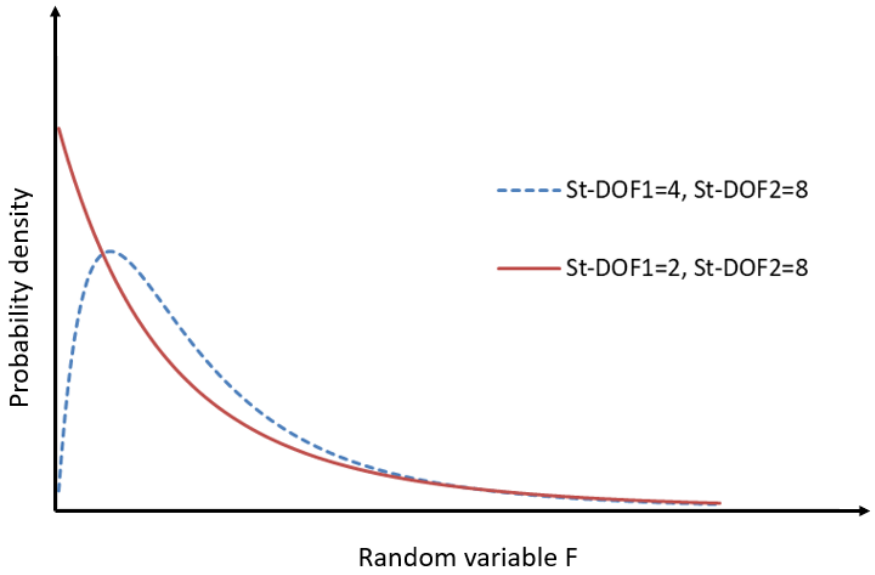

Figure 28. Fisher's F distribution for different degrees of freedom

Parallel to all the NHST framework, there is another important statistical tool that provides insight into data, the effect size. The p-value can answer the question: is there a statistically significant difference? On the other hand, effect size gives a measurement of a practical implication that is discipline specific. A widely used measurement of the effect size is Cohen's d (Eq. 2).

(2)

$$d = \frac{\bar{x}-\mu}{s}$$

The conventional standards for determining a small, medium or large effect are d=0.2 small, d=0.5 medium, d≥0.8 large. In this sense, even if the p-value (which depends on sample size) suggests that the difference between averages is not statistically significant, the effect size (independent of sample size) can suggest that there is a difference of practical importance.
A summary of statistical notations is included in Table 7 because the variables are similar to those used in structural engineering applications.

Table 8 Statistical variables

Variables	Interpretation
μ	True population mean
σ	True population standard deviation
s	Sample standard deviation
$\bar{x}$	Sample average (sample mean)
t	T-statistic

5.3.2 Identifying critical variables

The variables considered in this study are the following. SRA, a categorical variable that indicates the presence or absence of shrinkage reducing admixture in the concrete mix. Fibers, a categorical variable that indicates the presence or absence of polypropylene fibers in the concrete mix. IC, a categorical variable that indicates the presence or absence of lightweight fine aggregate to induce internal curing in the concrete mix. Finally, the variable aggregate is a categorical variable that considers two types of aggregate, limestone and granite. The single ring and dual ring tests are considered as two separate datasets because they are two separate tests. Conclusions are drawn individually for single ring and dual ring.

To start exploring the data, a single categorical linear regression model was fitted for every predictor variable. The models followed the form showed in Figure 29. A hypothesis test was performed on the slope coefficients (m) and the results are displayed in Table 8 and Table 9. For the variable of aggregate, the reference category was granite. The slope coefficient (difference in averages) obtained for the single ring dataset was 84.02 and the one obtained for the dual ring dataset was -21.62. These coefficients suggest conflicting effects: in the single ring test, the use of limestone appears to increase the time to cracking, while in the dual ring test, it appears to reduce it. However, both results are associated with high p-values (0.571 and 0.216), which are above the standard significance threshold (α=0.05). This indicates that the observed differences are not statistically significant. No reliable conclusion can be drawn about the effect of aggregate type based on this data alone. This aligns with findings in the literature, where studies have also reported inconsistent results, some favoring limestone (Aquino et al., 2010; X. Chen et al., 2012; Góra & Piasta, 2022), others favor granite (W. Chen et al., 2021; Golewski, 2024; Tufail et al., 2017).

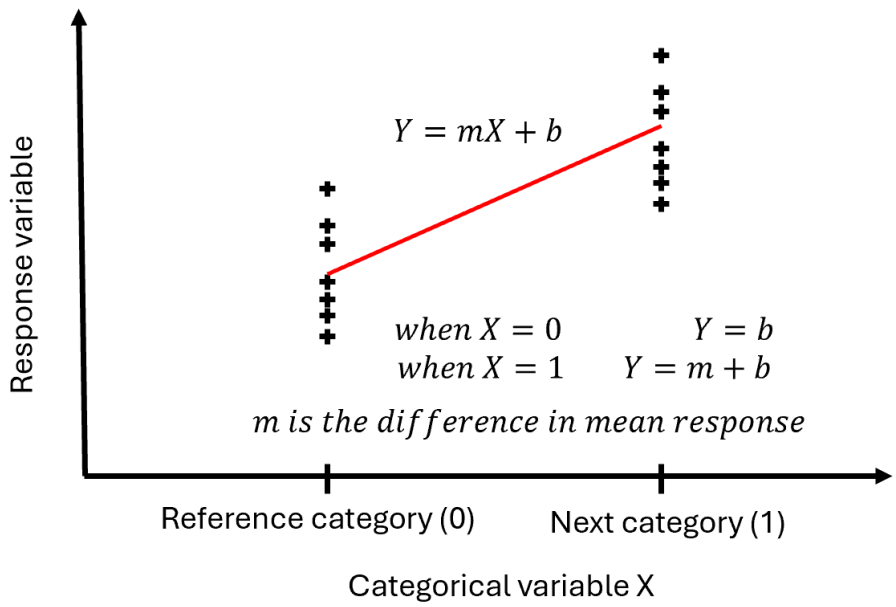

Figure 29. Linear regression with a categorical variable.

In the case of the predictor variable "fibers", the reference category was any specimen without fibers. For the single and dual ring testing, the t-statistics were t(31)=2.56 and t(33)=3.00, respectively. The number in parenthesis indicates the statistical degrees of freedom which define the shape of the probability distribution (see section 5.3.1). The associated p-values are 0.016 and 0.005, which are both below the significance level of α=0.05. In addition, the slope coefficients are nearly identical for both datasets (single ring 45.75 and dual ring 46.81). Taken together, the statistically significant p-values and consistent positive slopes indicate that the inclusion of fibers significantly increases the time to cracking in concrete.

Considering the internal curing, the reference category was the group without internal curing. Both single and dual-ring tests resulted in a positive slope coefficient, meaning that introducing internal curing to the concrete mixture extends the time until the first crack appears in the concrete. These results were found to be significant with t(31)=2.86, p=0.007 and t(33)=2.35, p=0.025 for single ring and dual ring, respectively.

For the categorical predictor of using shrinkage reducing admixtures, the reference category was the group without SRA. For the analysis of the single ring data, the addition of SRA was significant with t(31)=51.18, p=0.006. For the same test, the slope coefficient was 51.18, suggesting that adding SRA extends the time to cracking of concrete. On the other hand, for the dual ring test, the relation was found to be not significant with t(33)=1.68, p=0.103. It is important to note that effect size was calculated to be d=0.57, this corresponds to a Cohen's d, which is associated with a medium size effect of practical importance.

Table 9. Single linear regression results for single ring tests.

Predictor	Slope coefficient	T-statistic	P-value
Aggregate	84.02	0.57	0.571
Fibers	45.75	2.56	0.016
Internal Curing	50.17	2.86	0.007
SRA	51.18	2.94	0.006

*Statistical degrees of freedom are 31 for single ring.

Table 10. Single linear regression results for dual ring tests.

Predictor	Slope coefficient	T-statistic	P-value
Aggregate	-21.62	-1.26	0.216
Fibers	46.81	3.00	0.005
Internal Curing	38.26	2.35	0.025
SRA	28.36	1.68	0.103

*Statistical degrees of freedom are 33 for dual ring.

The variables that are statistically significant predictors of cracking time are SRA, fibers and internal curing, based on the linear regression models. In contrast, the variable aggregate type was not statistically significant, with p-values of 0.571 and 0.216 for single and dual ring tests, respectively. This suggests that using limestone or granite in the concrete did not produce consistent effects on the cracking time, and as such, this is not a good predictor of cracking time.

5.3.3 Multiple regression analysis

The most statistically significant variables found in section 1.2 were used to perform a two-way ANOVA analysis. In this type of analysis, a full linear model is considered of the form shown in Eq. (3). The equation includes two variables for simplicity and an explicit interaction term.

$$Y_i = m_1 X_{i1} + m_2 X_{i2} + m_3 X_{i1} X_{i2} + b \quad (3)$$

Results from this analysis are presented in Table 9 for single-ring testing and Table 10 for dual-ring testing. In general, the main effect of each single variable is significant, however, the interactions are not significant. This means that the combined effect of two variables on cracking time was not significantly different from the sum of their individual effects. In other

words, there is no evidence that one variable modifies or amplifies the effect of another. The lack of statistical significance instigated a new model that does not consider the interaction effects between groups is appropriate. Eight groups were formed: control, SRA, Fibers, IC (internal curing), SRA+Fiber, SRA+IC, Fiber+IC, and SRA+Fiber+IC and considered for a one-way ANOVA analysis.

Table 11. Results from two-way ANOVA for single-ring tests.

Effect	F-statistic	P-value
S2	15.96	0.0005
F8	13.62	0.001
LW	15.46	0.0006
F8 S2	1.638	0.212
LW S2	0.436	0.515
LW F8	1.174	0.289
LW F8 S2	0.028	0.869

Table 12. Results from two-way ANOVA for dual-ring tests.

Effect	F-statistic	P-value
S2	4.03	0.055
F8	11.42	0.002
LW	6.975	0.014
F8 S2	0.369	0.549
LW S2	0.384	0.541
LW F8	0.466	0.501
LW F8 S2	0.721	0.403

The results of the one-way ANOVA are presented in Table 11 and Table 12. Statistically significant results are obtained for both single and dual-ring tests. This indicates that there are significant differences among the eight groups created. Follow up tests comparing all groups were carried out.

Table 13. Results from one-way ANOVA for single-ring tests.

Predictor	Degrees of freedom	F-statistic	P-value
Between groups	65,346	6.90	0.0001
Within groups	33,812	6.90	0.0001

Table 14. Results from one-way ANOVA for dual-ring tests.

Predictor	Degrees of freedom	F-statistic	P-value
Between groups	42,207	3.48	0.009
Within groups	46,774	3.48	0.009

Given the small sample size after creating the eight groups mentioned, the metric of effect size was used over just looking at p-values for the follow-up tests.

As the number of combined methods increases, the number of samples within each group becomes smaller. For this reason, effect size is an additional resource for interpreting group differences. This approach allows us to better understand the practical importance of the results, especially in cases where p-values may not reflect the true magnitude of an effect due to limited data. The conventional standards (Cohen, 1988) for determining a small, medium, or large effect are: d=0.2 small, d=0.5 medium, d≥0.8 large.

Results for the effect sizes calculated for the group comparisons are presented in Table 13. If the effect size is positive, the first group (or right side) of “Comparison” column has the greatest average cracking time. On the other hand, if the effect size is negative, the second group (or left side) in the column “Comparison” has the greatest average cracking time. It is observed that all mitigation methods reduced cracking time effectively displaying medium to large effects.

It is remarkable that the single ring tests suggest the best method is to combine fibers with internal curing, with the close second method is the combination of SRA, fibers and internal curing. On the other hand, the dual ring dataset suggests that using only internal curing is just as effective as combining SRA, fibers and internal curing. In general, considering both tests agree that combining the three mitigation methods will have the most effective reduction in cracking. Figure 30 visually demonstrates the effect size of each variable.

Table 15. Effect sizes for multiple comparisons of mitigation methods.

Comparison	Single ring*	Dual ring*
Control S2	-1.45	-2.15
Control F8	-0.93	-2.08
Control LW	-0.58	-5.59
Control F8-S2	-1.82	-2.68
Control LW-S2	-1.94	-2.51
Control LW-F8	-3.44	-2.02
Control LW-F8-S2	-2.63	-5.56

*Note: the effect size indicates the normalized difference between the first group and the second group. If the value is positive, the first group would have a larger average cracking time. If the difference is negative, the second group has a larger average cracking time.

Figure 30. Effect size when compared to control group.

6 CONCLUSIONS AND RECOMMENDATIONS

6.1 Conclusions

A suite of single- and dual-ring specimens were evaluated to determine the time to cracking of three different mitigation measures and their combination. The following conclusions can be drawn:

- The incorporation of SRA has a negative effect on compressive strength, while tensile strength remains unaffected. Its addition helps mitigate cracking by delaying the time to crack formation.
- Based on laboratory results, limestone consistently performed better than granite in terms of cracking resistance, regardless of the mitigation measure used, while maintaining similar compressive strengths. The difference in behavior can be attributed to the lower water absorption and higher modulus of elasticity of limestone, that together contribute to reduced shrinkage. On the other hand, statistical analysis showed conflicting results, indicating that the effect of aggregate type was not significant and did not show a clear trend.
- Among individual mitigation methods, the replacement of aggregate with LWFA proved to be more efficient at delaying the cracking time up to 3 times the original cracking time for control mixtures. Statistical analysis showed that, after averaging across aggregate types, SRA performed better in the single-ring test, while LWFA was the most effective using dual-ring test.
- When combining two mitigation measures, the single-ring test showed SRA+IC as the best combination, while the dual-ring test did not show significant difference in average cracking time than when combining two mitigation measures.
- Internal curing using LWFA with fibers was the best combination of mitigation measures using the single-ring test, while the combination of SRA+F+LWFA also performed very well. In the dual-ring test, the best performance was achieved with the incorporation of LWFA, followed very closely by the combination of SRA+F+LWFA. Both of those combinations performed significantly better (up to 4 times) than the use of either SRA or F mitigation measures individually. This is true for laboratory results and statistical analysis.
- Both the single- and dual-ring tests are effective methods to measure cracking time. However, in this study, the single-ring test demonstrated greater efficiency, consistency, and repeatability. Dual-ring testing offers the ability to evaluate expansive agents as well.

The authors recommend using two of the three mitigation measures presented above in new concrete construction for bridge decks.

7 REFERENCES

AASHTO T334-08. (2020). *Standard Method of Test for Estimating the Cracking Tendency of Concrete*. American Association of State Highway and Transportation Officials.

AASHTO T363. (2017). *Standard Method of Test for Evaluating Stress Development and Cracking Potential due to Restrained Volume Change Using a Dual Ring Test*. American Association of State Highway and Transportation Officials.

Abousnina, R., Premasiri, S., Anise, V., Lokuge, W., Vimonsatit, V., Ferdous, W., & Alajarmeh, O. (2021). Mechanical Properties of Macro Polypropylene Fibre-Reinforced Concrete. *Polymers*, *13*(23), 4112. https://doi.org/10.3390/polym13234112

Aghaee, K., & Khayat, K. H. (2021). Effect Of Shrinkage-mitigating Materials On Performance Of Fiber-reinforced Concrete – An Overview. *Construction and Building Materials*, *305*, 124586. https://doi.org/10.1016/j.conbuildmat.2021.124586

Aghaee, K., & Khayat, K. H. (2023). Effect of internal curing and shrinkage-mitigating materials on microstructural characteristics of fiber-reinforced mortar. *Construction and Building Materials*, *386*, 131527. https://doi.org/10.1016/j.conbuildmat.2023.131527

Ahmad, J., Burduhos-Nergis, D. D., Arbili, M. M., Alogla, S. M., Majdi, A., & Deifalla, A. F. (2022). A Review on Failure Modes and Cracking Behaviors of Polypropylene Fibers Reinforced Concrete. *Buildings*, *12*(11), 1951. https://doi.org/10.3390/buildings12111951

Almusallam, A. A., Maslehuddin, M., Abdul-Waris, M., & Khan, M. M. (1998). Effect Of Mix Proportions On Plastic Shrinkage Cracking Of Concrete In Hot Environments. *Construction and Building Materials*, *12*(6–7), 353–358. https://doi.org/10.1016/S0950-0618(98)00019-1

Aquino, C., Inoue, M., Miura, H., Mizuta, M., & Okamoto, T. (2010). The effects of limestone aggregate on concrete properties. *Construction and Building Materials*, *24*(12), 2363–2368. https://doi.org/10.1016/j.conbuildmat.2010.05.008

Ashraf, W. B., & Noor, M. A. (2011). Performance-Evaluation of Concrete Properties for Different Combined Aggregate Gradation Approaches. *Procedia Engineering*, *14*, 2627–2634. https://doi.org/10.1016/j.proeng.2011.07.330

ASTM C33. (2024). *Standard Specification for Concrete Aggregates*. ASTM International.

ASTM C39. (2024). *Standard Test Method for Compressive Strength of Cylindrical Concrete Specimens*. ASTM International. https://doi.org/10.1520/C0039_C0039M-23

ASTM C127. (2024). *Standard Test Method for Relative Density (Specific Gravity) and Absorption of Coarse Aggregate*. ASTM International.

ASTM C128. (2022). *Standard Test Method for Relative Density (Specific Gravity) and Absorption of Fine Aggregate*. ASTM International.

ASTM C150/C150M. (2024). *Standard Specification for Portland Cement.* ASTM International.

ASTM C305. (2020). *Standard Practice for Mechanical Mixing of Hydraulic Cement Pastes and Mortars of Plastic Consistency*. ASTM International. https://doi.org/10.1520/C0305-20

ASTM C494. (2024). *Standard Specification for Chemical Admixtures for Concrete.* ASTM International.

ASTM C496. (2017). *Standard Test Method for Splitting Tensile Strength of Cylindrical Concrete Specimens*. ASTM International. https://doi.org/10.1520/C0496_C0496M-17

ASTM C1116/C1116M. (2023). *Standard Specification for Fiber-Reinforced Concrete.* ASTM International.

ASTM C1579. (2021). *Test Method for Evaluating Plastic Shrinkage Cracking of Restrained Fiber Reinforced Concrete (Using a Steel Form Insert)*. ASTM International. https://doi.org/10.1520/C1579-21

ASTM C1581. (2004). *Test Method for Determining Age at Cracking and Induced Tensile Stress Characteristics of Mortar and Concrete under Restrained Shrinkage*. ASTM International. https://doi.org/10.1520/C1581_C1581M-18A

ASTM C1761. (2023). *Specification for Lightweight Aggregate for Internal Curing of Concrete*. ASTM International. https://doi.org/10.1520/C1761_C1761M-23

ASTM F1684. (2021). *Specification for Iron-Nickel and Iron-Nickel-Cobalt Alloys for Low Thermal Expansion Applications*. ASTM International. https://doi.org/10.1520/F1684-06R21

Balendran, R. V., Zhou, F. P., Nadeem, A., & Leung, A. Y. T. (2002). Influence of steel fibres on strength and ductility of normal and lightweight high strength concrete. *Building and Environment*, *37*(12), 1361–1367. https://doi.org/10.1016/S0360-1323(01)00109-3

Banthia, N., & Gupta, R. (2006). Influence of polypropylene fiber geometry on plastic shrinkage cracking in concrete. *Cement and Concrete Research*, *36*(7), 1263–1267. https://doi.org/10.1016/j.cemconres.2006.01.010

Bentur, A., Igarashi, S., & Kovler, K. (2001). Prevention of autogenous shrinkage in high-strength concrete by internal curing using wet lightweight aggregates. *Cement and Concrete Research*, *31*(11), 1587–1591. https://doi.org/10.1016/S0008-8846(01)00608-1

Bentz, D. P., & Snyder, K. A. (1999). Protected paste volume in concrete: Extension to internal curing using saturated lightweight fine aggregate. *Cement and Concrete Research*, *29*(11), 1863–1867. https://doi.org/10.1016/S0008-8846(99)00178-7

Bolander, J. E. (2018). *Controlling Temperature and Shrinkage Cracks in Bridge Decks and Slabs*. California Department of Transportation.

Boshoff, W. P., & Combrinck, R. (2013). Modelling the severity of plastic shrinkage cracking in concrete. *Cement and Concrete Research*, 34–39.

Chen, W., Peng, L., & Yang, H. (2021). Fracture behaviors of concrete incorporating different levels of recycled coarse aggregate after exposure to elevated temperatures. *Journal of Building Engineering*, *35*, 102040. https://doi.org/10.1016/j.jobe.2020.102040

Chen, X., Yan, J. J., & Yang, H. Q. (2012). Influence of Aggregates on Cracking Sensitivity of Concrete. *Applied Mechanics and Materials*, *204–208*, 3299–3302. https://doi.org/10.4028/www.scientific.net/AMM.204-208.3299

Chilwesa, M., Akbarnezhad, A., Gharehchaei, M., Castel, A., Lloyd, R., & Foster, S. (2020). Using the Double Ring Test to Assess the Effect of Type of Aggregate Used on Thermal Cracking Potential of Concrete. In C. M. Wang, J. C. M. Ho, & S. Kitipornchai (Eds.), *ACMSM25* (Vol. 37, pp. 337–347). Springer Singapore. https://doi.org/10.1007/978-981-13-7603-0_34

Cohen, J. (1988). *Statistical Power Analysis for the Behavioral Sciences* (0 ed.). Routledge. https://doi.org/10.4324/9780203771587

De La Varga, I., Castro, J., Bentz, D., & Weiss, J. (2012). Application of Internal Curing forMixtures Containing High Volumes of Fly Ash. *Cement and Concrete Composites*, *34*(9), 1001–1008. https://doi.org/10.1016/j.cemconcomp.2012.06.008

De La Varga, I., Spragg, R., Muñoz, J., Helsel, M., & Graybeal, B. (2018). Cracking, Bond, and Durability Performance of Internally Cured Cementitious Grouts for Prefabricated Bridge Element Connections. *Sustainability*, *10*(11), 3881. https://doi.org/10.3390/su10113881

De La Varga, I., Spragg, R. P., El-Helou, R. G., & Graybeal, B. A. (2019, June 2). Shrinkage Cracking Propensity of UHPC. *Second International Interactive Symposium on UHPC*. Second International Interactive Symposium on UHPC. https://doi.org/10.21838/uhpc.9695

Dong, E., Yu, R., Fan, D., Chen, Z., & Ma, X. (2022). Absorption-desorption process of internal curing water in ultra-high performance concrete (UHPC) incorporating pumice: From relaxation theory to dynamic migration model. *Cement and Concrete Composites*, *133*, 104659. https://doi.org/10.1016/j.cemconcomp.2022.104659

Elzokra, A. A. E., Al Houri, A., Habib, A., Habib, M., & Malkawi, A. (2020). Shrinkage Behavior of Conventional and Nonconventional Concrete: A Review. *Civil Engineering Journal*, *6*(9), 1839–1851. https://doi.org/10.28991/cej-2020-03091586

Fujiwara, T. (2008). Effect of Aggregate on Drying Shrinkage of Concrete. *Journal of Advanced Concrete Technology*, *6*, 31–44.

Gangolu, A. R. (2001). Long-term Drying Shrinkage Of Mortar- Influence of Silica Fume And Size of Fine Aggregate. *Cement and Concrete Research*. https://doi.org/10.1016/S0008-8846(00)00347-1

Geiker, M. R., Bentz, D. P., & Jensen, O. M. (2004). Mitigating Autogenous Shrinkage by Internal Curing. *SP-218: High Performance Structural Lightweight Concrete*. SP-218: High Performance Structural Lightweight Concrete. https://doi.org/10.14359/13060

Gilbert, I. R., Castel, A., Khan, I., South, W., & Mohammadi, J. (2018). An Experimental Study of Autogenous and Drying Shrinkage. *High Tech Concrete: Where Technology and Engineering Meet*.

Golewski, G. L. (2024). Effect of Coarse Aggregate Type on the Fracture Toughness of Ordinary Concrete. *Infrastructures*, *9*(10), 185. https://doi.org/10.3390/infrastructures9100185

Góra, J., & Piasta, W. (2022). Test Results of the Modulus of Elasticity of Concretes with Various Coarse Aggregates and Standard Recommendations. *Advances in Science and Technology Research Journal*, *16*(6), 232–243. https://doi.org/10.12913/22998624/156583

Gribniak, V., Kaklauskas, G., & Baèinskas, D. (2007). State-of-art Review Of Shrinkage Effect On Cracking And Deformations Of Concrete Bridge Elements. *The Baltic Journal Of Road And Bridge Engineering*, *4*.

Guinea, G. V., El-Sayed, K., Rocco, C. G., Elices, M., & Planas, J. (2002). The effect of the bond between the matrix and the aggregates on the cracking mechanism and fracture parameters of concrete. *Cement and Concrete Research*, *32*(12), 1961–1970. https://doi.org/10.1016/S0008-8846(02)00902-X

Güneyisi, E., Gesoğlu, M., Mohamadameen, A., Alzeebaree, R., Algın, Z., & Mermerdaş, K. (2014). Enhancement of shrinkage behavior of lightweight aggregate concretes by shrinkage reducing admixture and fiber reinforcement. *Construction and Building Materials*, *54*, 91–98. https://doi.org/10.1016/j.conbuildmat.2013.12.041

Hannah, R. L., & Reed, S. E. (1992). *Strain Gage Users' Handbook*. Springer Science & Business Media.

Hasan, N. (2020). *Durability and Sustainability of Concrete: Case Studies for Concrete exposures*. Springer International Publishing. https://doi.org/10.1007/978-3-030-51573-7

Holt, E. (2001). *Early age autogenous shrinkage of concrete*. University of Washington.

Holt, E. (2005). Contribution of mixture design to chemical and autogenous shrinkage of concrete at early ages. *Cement and Concrete Research*, 464–472.

Holt, E., & Leivo, M. (2004). Cracking risks associated with early age shrinkage. *Cement and Concrete Composites*, *26*(5), 521–530. https://doi.org/10.1016/S0958-9465(03)00068-4

Houst, Y. (1997). Carbonation shrinkage of hydrated cement paste. *4th CANMET/ACI International Conference on Durability of Concrete*, 481–491.

Hwang, E., Kim, G., Koo, K., Moon, H., Choe, G., Suh, D., & Nam, J. (2021). Compressive Creep and Shrinkage of High-Strength Concrete Based on Limestone Coarse Aggregate Applied to High-Rise Buildings. *Materials*, *14*(17), 5026. https://doi.org/10.3390/ma14175026

Hyodo, H., Tanimura, M., Sato, R., & Kawai, K. (2013). Evaluation of Effect of Aggregate Properties on Drying Shrinkage of Concrete. *Third International Conference on Sustainable Construction Materials and Technologies*.

Idiart, A., Bisschop, J., Caballero, A., & Lura, P. (2012). A numerical and experimental study of aggregate-induced shrinkage cracking in cementitious composites. *Cement and Concrete Research*, *42*(2), 272–281. https://doi.org/10.1016/j.cemconres.2011.09.013

Karagüler, M. E., & Yatağan, M. S. (2018). Effect of aggregate size on the restrained shrinkage of the concrete and mortar. *MOJ Civil Engineering*.

Kioumarsi, M., Azarhomayun, F., Haji, M., & Shekarchi, M. (2020). Effect of Shrinkage Reducing Admixture on Drying Shrinkage of Concrete with Different w/c Ratios. *Materials*, *13*(24), 5721. https://doi.org/10.3390/ma13245721

Klemczak, B., Batog, M., Pilch, M., & Zmij, A. (2017). Analysis of Cracking Risk in Early Age Mass Concrete with Different Aggregate Types. *International Conference on Analytical Models and New Concepts in Concrete and Masonry Structures AMCM'2017*, 234–241.

Kohno, K., Okamoto, T., Isikawa, Y., Sibata, T., & Mori, H. (1999). Effects of artificial lightweight aggregate on autogenous shrinkage of concrete. *Cement and Concrete Research*, *29*(4), 611–614. https://doi.org/10.1016/S0008-8846(98)00202-6

Kosmatka, S. H., & Wilson, M. L. (2011). *Design and Control of Concrete Mixtures* (15th ed.). Portland Cement Association.

Kozul, R., & Darwin, D. (1997). *Effects of Aggregate Type, Size, and Content on Concrete Strength and Fracture Energy*. University of Kansas Center for Research, INC.

Kurup, D. S., Mohan, M. K., Van Tittelboom, K., De Schutter, G., Santhanam, M., & Rahul, A. V. (2024). Early-age shrinkage assessment of cementitious materials: A critical review. *Cement and Concrete Composites*, *145*, 105343. https://doi.org/10.1016/j.cemconcomp.2023.105343

Langer, W. H. (2011). *Aggregate resource availability in the conterminous United States, including suggestions for addressing shortages, quality, and environmental concerns* (Report 2011–1119; Open-File Report). USGS Publications Warehouse. https://doi.org/10.3133/ofr20111119

Latifi, M. R., Biricik, Ö., & Mardani Aghabaglou, A. (2022). Effect of the addition of polypropylene fiber on concrete properties. *Journal of Adhesion Science and Technology*, *36*(4), 345–369. https://doi.org/10.1080/01694243.2021.1922221

Liu, J., Shi, C., Ma, X., Khayat, K. H., Zhang, J., & Wang, D. (2017). An overview on the effect of internal curing on shrinkage of high performance cement-based materials. *Construction and Building Materials*, *146*, 702–712. https://doi.org/10.1016/j.conbuildmat.2017.04.154

Lofgren, I., & Esping, O. (2006). Early Age Cracking of Self-Compacting Concrete. *International RILEM Conference on Volume Changes of Hardening Concrete: Testing and Mitigation*.

Luhr, S. (2015). Wyoming's Construction Aggregate Resource. *Wyoming State Geological Survey*.

Lura, P., Bentz, D. P., Lange, D. A., Kovler, K., & Bentur, A. (2004). Pumice aggregates for internal water curing. *Proceedings of International RILEM Symposium on Concrete Science and Engineering: A Tribute to Arnon Bentur*, 22–24.

Lura, P., Pease, B., Mazzotta, G. B., Rajabipour, F., & Weiss, J. (2007). Influence of Shrinkage-Reducing Admixtures on Development of Plastic Shrinkage Cracks. *ACI Materials Journal*, 187–194.

Maia, L., Figueiras, H., Nunes, S., Azenha, M., & Figueiras, J. (2012). Influence of shrinkage reducing admixtures on distinct SCC mix compositions. *Construction and Building Materials*, 304–312.

Matalkah, F., Salem, T., Shaafaey, M., & Soroushian, P. (2019). Drying shrinkage of alkali activated binders cured at room temperature. *Construction and Building Materials*, 563–570.

Meininger, R. C. (1966). *Drying Shrinkage of Concrete*. National Ready Mixed Concrete Association.

Mendoza, C., Aire, C., & Davila, P. (2011). Influencia de las fibras de polipropileno en las propiedades del concreto en estados plastico y endurecido. *Concreto y Cemento*, *2*(2), 35–47.

Micro-Measurements. (2014). TN-504-1. *Strain Gage Thermal Output and Gage Factor Variation with Temperature*.

Myers, D., Kang, T. H. K., & Ramseyer, C. (2008). Early-Age Properties of Polymer Fiber-Reinforced Concrete. *International Journal of Concrete Structures and Materials*, 9–14.

Naaman, A. E., Wongtanakitcharoen, T., & Hauser, G. (2005). Influence of Different Fibers on Plastic Shrinkage Cracking of Concrete. *ACI Materials Journal*, *102*(1), 49–58. ProQuest One Academic; SciTech Premium Collection.

Nakamoto, J., Masaki, R., & Takagi, K. (2012). Influence of Coarse Aggregate on Drying Shrinkage of Concrete. *Journal of the Society of Materials Science, Japan*, 819–824.

Oliveira, M., Ribeiro, A., & Branco, F. (2014). Combined effect of expansive and shrinkage reducing admixtures to control autogenous shrinkage in self-compacting concrete. *Construction and Building Materials*, 267–275.

Pease, B., Weiss, W. J., & Shah, H. (2005). *Restrained shrinkage behavior of mixtures containing shrinkage reducing admixtures and fibers*.

Pillar, N. M. P., & Repette, W. L. (2015). The effect of fibers on the loss of water by evaporation and shrinkage of concrete. *Ibracon Structures and Materials Journal*, 8–13.

Powers, T. C. (1959). Causes and Control of Volume Change. *Journal PCA Research Laboratories*, 29–39.

Qi, C., Weiss, J., & Olek, J. (2003). Characterization of plastic shrinkage cracking in fiber reinforced concrete using image analysis and a modified Weibull function. *Materials and Structures*, 386–395.

Ramujee, K. (2013). Strength Properties Of Polypropylene Fiber Reinforced Concrete. *International Journal of Innovative Research in Science, Engineering and Technology*, *2*(8).

Raoufi, K., Schlitter, J., Bentz, D., & Weiss, J. (2011). Parametric Assessment of Stress Development and Cracking in Internally Cured Restrained Mortars Experiencing Autogenous Deformations and Thermal Loading. *Advances in Civil Engineering*, *2011*, 1–16. https://doi.org/10.1155/2011/870128

Şahmaran, M., Lachemi, M., Hossain, K. M. A., & Li, V. C. (2009). Internal curing of engineered cementitious composites for prevention of early age autogenous shrinkage cracking. *Cement and Concrete Research*, *39*(10), 893–901. https://doi.org/10.1016/j.cemconres.2009.07.006

Sakata, K., & Shimomura, T. (2004). Recent Progress in Research on and Code Evaluation of Concrete Creep and Shrinkage in Japan. *Journal of Advanced Concrete Technology*, 133–140.

Schlitter, J., Henkensiefken, R., Castro, J., Raoufi, K., & Weiss, J. (2010). *Development of Internally Cured Concrete for Increased Service Life*. Joint Transportation Research Program.

Shen, P., Lu, J.-X., Lu, L., He, Y., Wang, F., & Hu, S. (2021). An alternative method for performance improvement of ultra-high performance concrete by internal curing: Role of physicochemical properties of saturated lightweight fine aggregate. *Construction and Building Materials*, *312*, 125373. https://doi.org/10.1016/j.conbuildmat.2021.125373

Shh, S. P., Krguller, M. E., & Sarigaphuti, M. (1992). Effects of Shrinkage-Reducing Admixtures on Restrained Shrinkage Cracking of Concrete. *Materials Journal*, 289–295.

Sofi, M., Baweja, D., Mendis, P., & Elvira, E. (2014). Anchorage zones behaviour of early age concrete: Application to post-tensioned members. *Construction and Building Materials*, 1–12.

Takada, K., Van Breugel, K., Koenders, E. A. B., & Kaptijn, N. (1999). 15 EXPERIMENTAL EVALUATION OF AUTOGENOUS SHRINKAGE OF LIGHTWEIGHT AGGREGATE CONCRETE. *Autogenous Shrinkage of Concrete: Proceedings of the International Workshop, Organised by JCI (Japan Concrete Institute), Hiroshima, June 13-14, 1998*, 229.

Tang, S., Huang, D., & He, Z. (2021). A review of autogenous shrinkage models of concrete. *Journal of Building Engineering*.

Tangtermsirikul, S., & Tatong, S. (2001). Modeling of Aggregate Stiffness and Its Effect on Shrinkage of Concrete. *ScienceAsia*, 185–192.

Tazawa, E., & Miyazawa, S. (1995). Experimental Study on Mechanism of Autogenous Shrinkage of Concrete. *Cement and Concrete Research*, 1633–1638.

Tremper, B., & Spellman, D. L. (1963). *Shrinkage of Concrete-Comparison of Laboratory and Field Performance*. Highway Research Record No. 3.

Tufail, M., Shahzada, K., Gencturk, B., & Wei, J. (2017). Effect of Elevated Temperature on Mechanical Properties of Limestone, Quartzite and Granite Concrete. *International*

Journal of Concrete Structures and Materials, *11*(1), 17–28. https://doi.org/10.1007/s40069-016-0175-2

Van Breugel, K. (1998). Prediction of Temperature Development in Hardening Concrete. *Rilem Report 15*, 51–57.

Wang, H., An, D., Nie, F., Zhao, H., & Xu, C. (2023). Prediction of Restrained Shrinkage of New-to-old Concrete Interface. *Periodica Polytechnica Civil Engineering*, *68*(1), 131–140. https://doi.org/10.3311/PPci.22430

Wang, J.-Y., Banthia, N., & Zhang, M.-H. (2012). Effect of shrinkage reducing admixture on flexural behaviors of fiber. *Cement & Concrete Composites*, 443–450.

Wang, J.-Y., Chia, K.-S., Richard Liew, J.-Y., & Zhang, M.-H. (2013). Flexural performance of fiber-reinforced ultra lightweight cement. *Cement & Concrete Composites*, 39–47.

Wei, J., Farzadnia, N., & Khayat, K. H. (2024). Synergistic effect of macro synthetic fiber and shrinkage-reducing admixture on engineering properties of fiber-reinforced super-workable concrete. *Construction and Building Materials*, *414*, 134566. https://doi.org/10.1016/j.conbuildmat.2023.134566

Weiss, J. (2022). *Guidance to Reduce Shrinkage and Restrained Shrinkage Cracking*. National Concrete Pavement Technology Center.

White, G. R. (1975). *Basic Concrete Construction Practices*. Portland Cement Association.

Wilson, C., & Weiss, J. (2020). Improving the Durability of High Early Strength (HES) Concrete Patching Materials for Concrete Pavements. *Transportation Research Records*, 12–23.

Woyciechowski, P., Chilmon, K., & Sokołowska, J. J. (2016). Effect of limestone and granite coarse aggregate on drying shrinkage of a concrete. *MATEC Web of Conferences*, *86*, 04015. https://doi.org/10.1051/matecconf/20168604015

Wu, L., Farzadnia, N., Shi, C., Zhang, Z., & Wang, H. (2017). Autogenous shrinkage of high performance concrete: A review. *Construction and Building Materials*, 62–75.

Xi, Y., Shing, B., Abu-Hejleh, N., Asiz, A., Suwito, A., Xie, Z., & Ababneh, A. (2003). *Assesment of the cracking problem in newly constructed bridge decks in Colorado*. Colorado Department of Transportation Research Branch.

Xu, Y., & Chung, D. D. L. (2000). Reducing the drying shrinkage of cement paste by admixture surface treatments. *Cement and Concrete Research*, 241–245.

Yang, L., Ma, X., Liu, J., Hu, X., Wu, Z., & Shi, C. (2022). Improving the effectiveness of internal curing through engineering the pore structure of lightweight aggregates. *Cement and Concrete Composites*, *134*, 104773. https://doi.org/10.1016/j.cemconcomp.2022.104773

Yang, L., Shi, C., Liu, J., & Wu, Z. (2021). Factors affecting the effectiveness of internal curing: A review. *Construction and Building Materials*, *267*, 121017. https://doi.org/10.1016/j.conbuildmat.2020.121017

Ye, H., Radlińska, A., & Neves, J. (2017). Drying and carbonation shrinkage of cement paste containing alkalis. *Materials and Structures*, *50*(2), 132. https://doi.org/10.1617/s11527-017-1006-x

Yoo, D.-Y., Kim, J., Zi, G., & Yoon, Y.-S. (2015). Effect of shrinkage-reducing admixture on biaxial flexural behavior of ultra-high-performance fiber-reinforced concrete. *Construction and Building Materials*, 67–75.

Yousefieh, N., Joshaghani, A., Hajibandeh, E., & Shekarchi, M. (2017). Influence of fibers on drying shrinkage in restrained concrete. *Construction and Building Materials*, *148*, 833–845. https://doi.org/10.1016/j.conbuildmat.2017.05.093

Zhan, P., & He, Z. (2019a). Application of Shrinkage Reducing Admixture in Concrete: A Review. *Construction and Building Materials*, 676–690.

Zhan, P., & He, Z. (2019b). Application of Shrinkage Reducing Admixture in Concrete: A Review. *Construction and Building Materials*, 676–690.

Zhang, G., Luo, X., Liu, Y., & Zhu, Z. (2018). Influence of Aggregates on Shrinkage-Induced Damage in Concrete. *Journal of Materials in Civil Engineering*, *30*(11), 04018281. https://doi.org/10.1061/(ASCE)MT.1943-5533.0002329

Zhang, M., Gao, S., Liu, T., Guo, S., & Zhang, S. (2024). High-Performance Materials Improve the Early Shrinkage, Early Cracking, Strength, Impermeability, and Microstructure of Manufactured Sand Concrete. *Materials*, *17*(10), 2465. https://doi.org/10.3390/ma17102465

Zhang, W., Zakaria, M., & Hama, Y. (2013). Influence of aggregate materials characteristics on the drying shrinkage properties of mortar and concrete. *Construction and Building Materials*, 500–510.

Zhutovsky, S., Kovler, K., & Bentur, A. (2002). Efficiency of lightweight aggregates for internal curing of high strength concrete to eliminate autogenous shrinkage. *Materials and Structures*, *35*, 97–101.

Zhutovsky, S., Kovler, K., & Bentur, A. (2004). Influence of cement paste matrix properties on the autogenous curing of high-performance concrete. *Cement and Concrete Composites*, *26*(5), 499–507. https://doi.org/10.1016/S0958-9465(03)00082-9

APPENDICES

Selected strain graphs are shown here to illustrate the results.

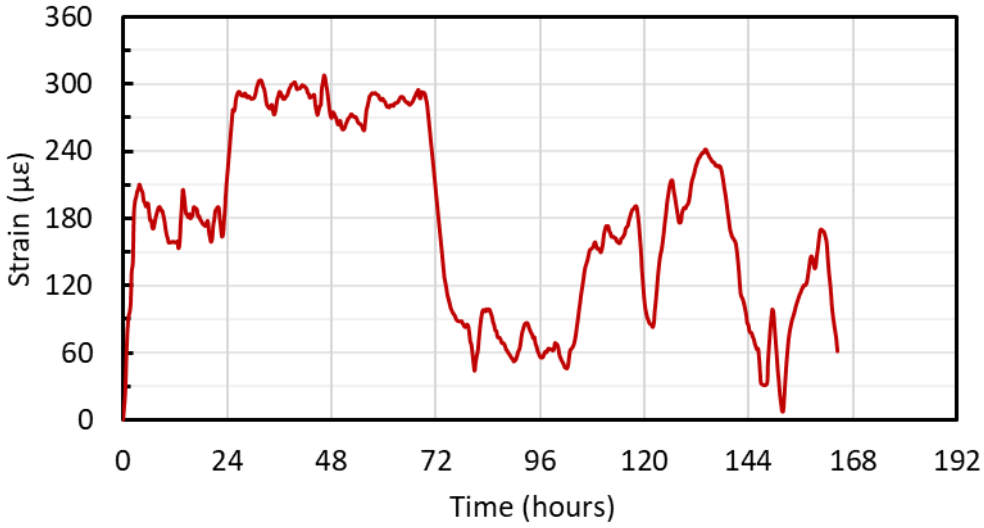

A1. SR-GR-CONTROL

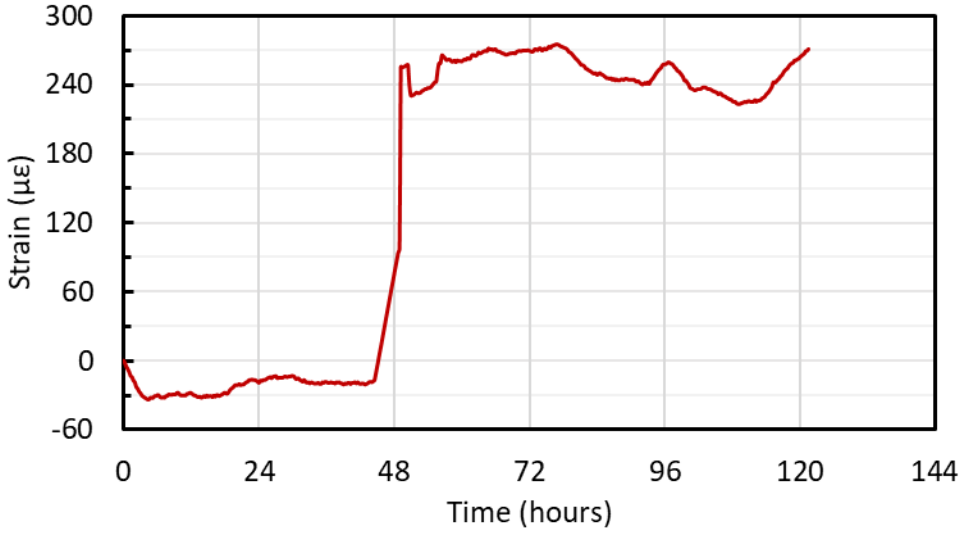

A2. SR-GR-SRA

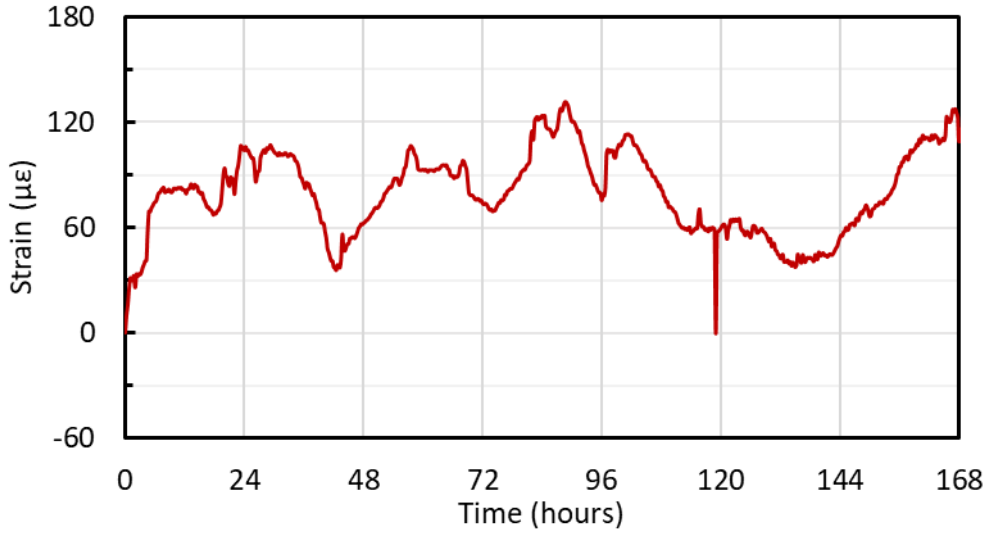

A3. SR-LS-LW+SRA

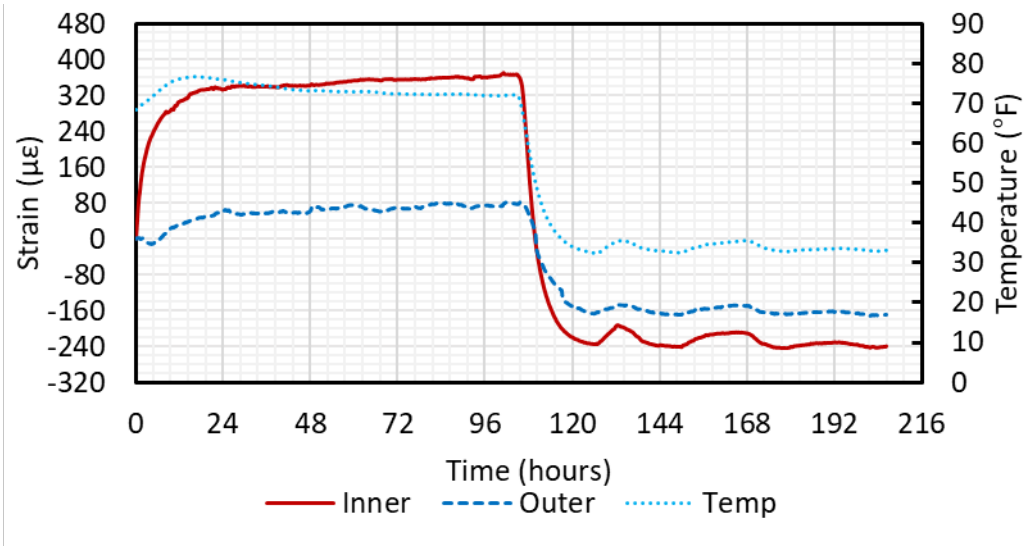

A4.DR-FR-F

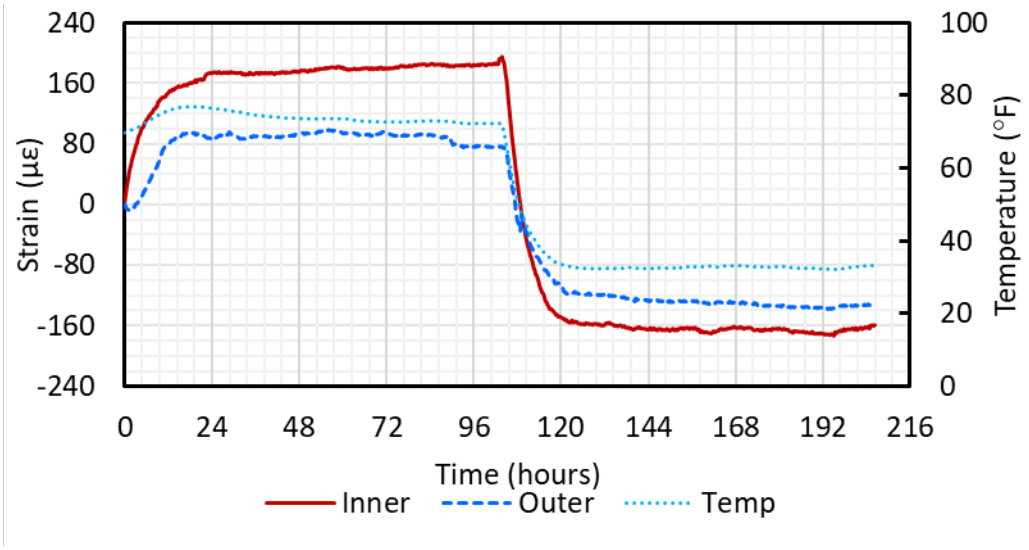

A5. DR-GR-SRA

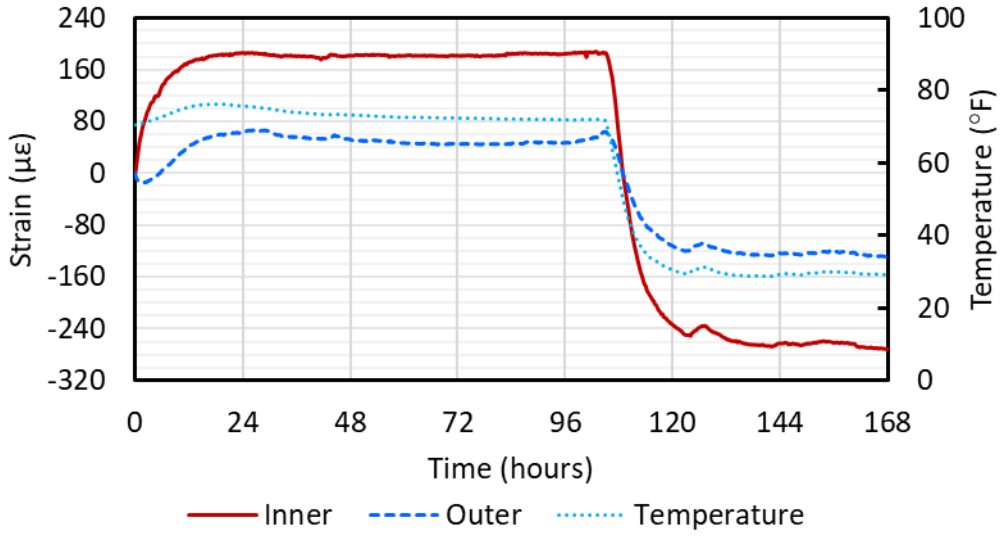

A6. DR-LS-F+SRA